NAVAL POSTGRADUATE SCHOOL

MONTEREY, CALIFORNIA

THESIS

STUDY OF A NOVEL IONIZER CONFIGURATION FOR THE ION THRUSTER

by

Jason Theodore Cooper

December 2006

Thesis Advisor: Oscar Biblarz
Co-Advisor: Jose Sinibaldi

Approved for public release; distribution is unlimited

THIS PAGE INTENTIONALLY LEFT BLANK

REPORT DOCUMENTATION PAGE			Form Approved OMB No. 0704-0188

1. AGENCY USE ONLY *(Leave blank)*	2. REPORT DATE December 2006	3. REPORT TYPE AND DATES COVERED Master's Thesis

4. TITLE AND SUBTITLE Study of a Novel Ionizer Configuration for the Ion Thruster	5. FUNDING NUMBERS
6. AUTHOR(S) Jason Theodore Cooper	
7. PERFORMING ORGANIZATION NAME(S) AND ADDRESS(ES) Naval Postgraduate School Monterey, CA 93943-5000	**8. PERFORMING ORGANIZATION REPORT NUMBER**
9. SPONSORING /MONITORING AGENCY NAME(S) AND ADDRESS(ES) N/A	**10. SPONSORING/MONITORING AGENCY REPORT NUMBER** N/A

11. SUPPLEMENTARY NOTES The views expressed in this thesis are those of the author and do not reflect the official policy or position of the Department of Defense or the U.S. Government.

12a. DISTRIBUTION / AVAILABILITY STATEMENT Approved for public release; distribution is unlimited	12b. DISTRIBUTION CODE A

13. ABSTRACT (maximum 200 words)

Micro-satellites often require the adaptation of existing propulsion systems. Electric propulsion thrusters are perhaps the best candidates to meet these needs and ion engines are among the most scalable. Miniaturizing the ion engine will require novel concepts for the ionizer with perhaps novel propellants. MEMS, nanotechnology and other technological advances are expected to impact on new designs.

Our work shows that the ionization of Argon, which is an alternate fuel to Xenon, can be achieved at low voltages by utilizing Micro-Structured Electrode (MSE) Arrays. Copper-clad sheets separated by a dielectric material (fiberglass laminate epoxy resin system combined with a glass fabric substrate) of varying thickness (0.1 mm to 0.4 mm) form the discharge electrodes in the MSE arrays The wafers are drilled with an array of holes and this geometry serves to concentrate the electric field between electrodes enhancing electron emission at the cathode. Minimum breakdown voltages between 240 and 280 Volts at pressures of around 100 mTorr ($0.133 N/m^2$) were consistently obtained with arrays of hole diameter ranging from 300 to 500μm. These results are consistent with conventional Paschen-curves with two empirical constants that arise from our unconventional geometrical arrangements and from the different material properties.

14. SUBJECT TERMS Ion Propulsion, Ion Engine, MSE array, Paschen Curve, Ionizer	15. NUMBER OF PAGES 81
	16. PRICE CODE

17. SECURITY CLASSIFICATION OF REPORT	18. SECURITY CLASSIFICATION OF THIS PAGE	19. SECURITY CLASSIFICATION OF ABSTRACT	20. LIMITATION OF ABSTRACT
Unclassified	Unclassified	Unclassified	UL

NSN 7540-01-280-5500

Standard Form 298 (Rev. 2-89)
Prescribed by ANSI Std. 239-18

THIS PAGE INTENTIONALLY LEFT BLANK

Approved for public release; distribution is unlimited

STUDY OF A NOVEL IONIZER CONFIGURATION FOR ION THRUSTERS

Jason Theodore Cooper
Lieutenant, United States Navy
B.S., Washington State University, 1996

Submitted in partial fulfillment of the
requirements for the degree of

MASTER OF SCIENCE IN ASTRONAUTICAL ENGINEERING

from the

NAVAL POSTGRADUATE SCHOOL
December 2006

Author: Jason T. Cooper

Approved by: Oscar Biblarz
Thesis Advisor

Jose O. Sinibaldi
Co-Advisor

Anthony J. Healey
Chairman, Department of Mechanical and Astronautical Engineering

THIS PAGE INTENTIONALLY LEFT BLANK

ABSTRACT

Micro-satellites often require the adaptation of existing propulsion systems. Electric propulsion thrusters are perhaps the best candidates to meet these needs and ion engines are among the most scalable. Miniaturizing the ion engine will require novel concepts for the ionizer with perhaps novel propellants. MEMS, nanotechnology and other technological advances are expected to impact on new designs.

Our work shows that the ionization of Argon, which is an alternate fuel to Xenon, can be achieved at low voltages by utilizing Micro-Structured Electrode (MSE) Arrays. Copper-clad sheets separated by a dielectric material (fiberglass laminate epoxy resin system combined with a glass fabric substrate) of varying thickness (0.1 mm to 0.4 mm) form the discharge electrodes in the MSE arrays The wafers are drilled with an array of holes and this geometry serves to concentrate the electric field between electrodes enhancing electron emission at the cathode. Minimum breakdown voltages between 240 and 280 Volts at pressures of around 100 mTorr ($0.133 N/m^2$) were consistently obtained with arrays of hole diameter ranging from 300 to 500μm. These results are consistent with conventional Paschen-curves with two empirical constants that arise from our unconventional geometrical arrangements and from the different material properties.

THIS PAGE INTENTIONALLY LEFT BLANK

TABLE OF CONTENTS

LIST OF FIGURES

THIS PAGE INTENTIONALLY LEFT BLANK

LIST OF TABLES

THIS PAGE INTENTIONALLY LEFT BLANK

ACKNOWLEDGMENTS

I would like to take the opportunity to thank the following individuals:

Dr. Leonard Ferrari for approving the initial $5,000 research funds to initiate this research effort; Dr. Gamani Karunasiri for providing the bell-jar and vacuum system; Messiers Don Snyder, Samuel Barone, and George Jaksha of the Physics Department for their invaluable technical assistance; Professors Oscar Biblarz and Jose Sinibaldi for their knowledge and guidance; LT Frank Perry Jr. for his support and tolerance as my thesis and lab partner, and last but not least my loving wife Sarah Ann who has been a godsend in her devotion and support of me.

Without the support of these people none of this would have been possible.

THIS PAGE INTENTIONALLY LEFT BLANK

I. INTRODUCTION

A. ION ENGINE HISTORY

The theories behind ion engines have been attributed to the German scientist Dr. Wernher von Braun during the 1930s. At this time, the German military was more interested in weapons of war than interplanetary rockets, so his theories remained untested until the end of World War II, when he and hundreds of fellow scientists were brought to the United States. Once in the US, they were able to develop their theories enough that in 1958, the Army Ballistic Missile Agency initiated a contract with Electro-Optical Systems to study ion propulsion. The result of this was a 0.1 pound-thrust engine developed by Hughes Research Laboratory before it stopped due to the Apollo program [8, 9].

In the early 1990s, the NASA Solar Electric Power Technology Applications Readiness project revived the Hughes ion thruster. This project began to study the idea of using a Xenon propellant within an ion engine. In 1996 one such engine was built and fired for over 8000 hours, making the test a success. Deep Space I was a small space craft that was launched onboard a small Delta II rocket from Cape Canaveral Air Station, Florida on October 24, 1998. The propulsion system managed to propel the craft at a rate where it could sometimes travel at 750,000 miles per day. After the scheduled end of the test, the mission was extended for the opportunity to fly close to the comet Borrelly, and take some of the best pictures to date [8].

B. ION ENGINE THEORY

Modern ion thrusters use inert gases for the propellant. The majority of these thrusters use Xenon, which is chemically inert, colorless, odorless, and tasteless. The propellant is injected upstream of the thruster and flows to the downstream end. This injection method is preferred because it increases the time that the propellant remains in the chamber thereby ensuring higher ionization efficiencies [9].

In a basic ion thruster, electrons are created at a hollow cathode, called the discharge cathode, located at the center of the engine on the upstream end. The electrons

flow out of the discharge cathode and are attracted to the discharge chamber walls, which are charged to a high positive potential by the thruster's power supply.

The electrons from the discharge cathode ionize the propellant by means of electron bombardment. High-strength magnets are placed along the discharge chamber walls so that as electrons approach the walls, they are redirected into the discharge chamber by the magnetic fields. By maximizing the length of time that electrons and propellant atoms remain in the discharge chamber, the chance of ionization is maximized, which makes the ionization process as efficient as possible at these low pressures.

In an ion thruster, ions are accelerated by electrostatic forces. The electric fields used for acceleration are generated by electrodes positioned at the downstream end of the thruster. Each set of electrodes, called ion optics or grids, contains thousands of coaxial apertures. Each set of apertures acts as a lens that electrically focuses ions through the optics.

Most ion thrusters use a two-electrode system, where the upstream electrode is charged highly positive, and the downstream electrode is charged highly negative. Since the ions are generated in a region of high positive charge and the accelerator grid's potential is negative, the ions are attracted toward the accelerator grid and are focused out of the discharge chamber through the apertures, creating thousands of ion jets. The stream of all the ion jets together is called the ion beam. The thrust force is the change of momentum to the ions produced by the accelerator grid. The exhaust velocity of the ions in the beam is proportional to the voltage applied to the optics.

Because the ion thruster produces a large amount of positive ions, an equal amount of negative charge must be expelled to keep the total charge of the exhaust beam neutral. A second hollow cathode called the neutralizer is located on the downstream perimeter of the thruster and expels the needed electrons as depicted in Figure 1.

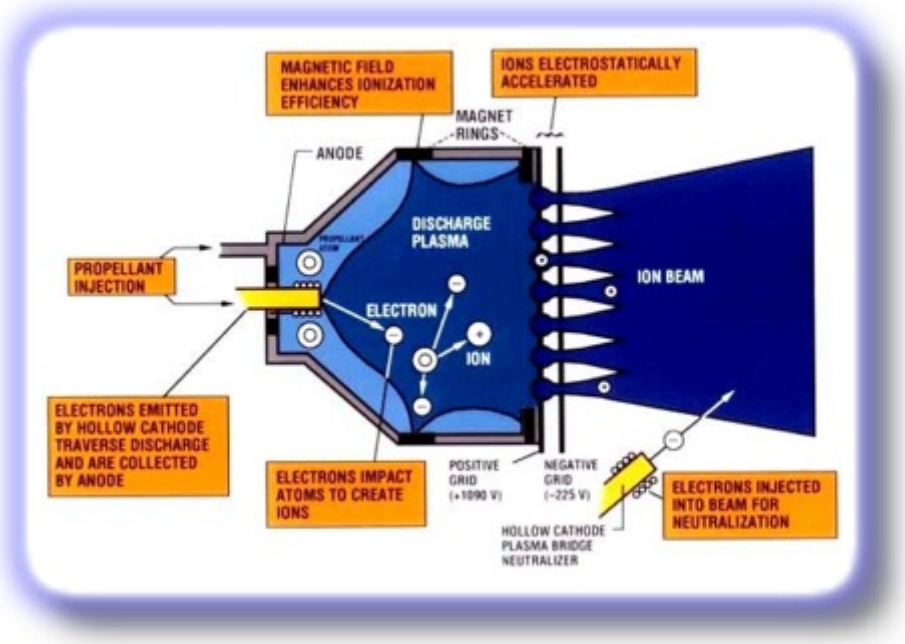

Figure 1. Ion thruster operation (From Ref. 9)

The ion propulsion system consists of five main parts: the power source, power processing unit, propellant management system, the control computer, and the ion thruster. The ion propulsion system power source can be any source of electrical power, but solar and nuclear are the primary options. A solar electric propulsion system uses sunlight and solar cells for power generation. A nuclear electric propulsion system uses a nuclear heat source coupled to an electric generator. The power processing unit converts the electrical power generated by the power source into the power required for each component of the ion thruster. It generates the voltages required by the ion optics and discharge chamber and the high currents required for the hollow cathodes. The propellant management system controls the propellant flow from the propellant tank to the thruster and hollow cathodes [9].

The control computer controls and monitors system performance. The ion thruster then processes the propellant and power to perform work. Modern ion thrusters are capable of propelling a spacecraft up to 90,000 meters per second (about 200,000 miles per hour). The tradeoff for this high top speed is low thrust (or low acceleration) [9].

Modern ion thruster units can deliver up to 0.5 N of thrust. To compensate for low thrust, the ion thruster must be operated for a long time for the spacecraft to reach its desired speed. Because ion thrusters use inert gas for propellant, they eliminate the risk of explosions associated with chemical propulsion. The usual propellant is Xenon, but other gases such as Krypton and Argon may be used [9].

C. FIELDS COVERED

Ion propulsion is one of several propulsion methods utilized for orbital maintenance of spacecraft as well as interplanetary applications. With the advent of the Hall thruster, ion propulsion technology is beginning to take a back seat in research as Hall Effect technology is more readily adaptable to different applications, however, ion propulsion technologies should not be ignored. Current ion technology utilizes Xenon as the propellant of choice due to its high atomic mass, which as the mass is increased so is the momentum change and thus the net thrust. Unfortunately, Xenon is quite expensive. If more common elements such as Argon could be used the price of the propellant would become much cheaper [4].

Another problem with current ion engine technologies is that they have reached size limitations with current technologies. To make ion engines a viable alternative to other propulsion methods they must be scalable beyond where they are now. A possible approach to this would be the use of Micro Structured Electrode (MSE) Arrays [6]. This would reduce or even eliminate the ionization chamber of current engines allowing huge mass and size savings. It would also allow the engines to be scaled to much smaller sizes for applications such as micro satellite propulsion. Another benefit of utilizing MSE Arrays is the reduction in power requirements. Typical ion engines operate in the kilowatt range but by redesigning the technology to use MSE arrays the power requirements would drop to the range of hundreds of watts and at only a few hundred volts, thus requiring less power generation and a smaller spacecraft power bus.

This thesis is concerned with utilizing MSE arrays to modify the design of the ionizer section. Different configurations of MSE arrays are studied in a wide pressure range from 10 milli-Torr to 1 Torr (or 0.122289 N/m^2 to 133.289 N/m^2). The configurations studied involved materials and design, the type of insulator and the structure diameters.

The MSE arrays were studied with respect to the electrical characteristics of the materials and the gas.

The second chapter covers the test equipment setup used to for the experiments and offers a description of the MSE wafers. The third chapter covers ion engine theory, both current ion engine configurations and MSE array theory. The MSE array theory will cover the breakdown process at various pressures and the mechanisms for generating sustained discharges. The fourth chapter will cover the data and results of the simulations and testing of the MSE arrays. The fifth and sixth chapters will draw conclusions based on those results and recommendations for future studies. The thesis of LT Frank Perry compliments this effort [7].

The ultimate purpose of this research is to explore the use of MSE arrays as a viable alternative to the present ionizing chambers in the ion propulsion system.

THIS PAGE INTENTIONALLY LEFT BLANK

II. EXPERIMENTAL APPARATUS

A. VACUUM CHAMBER AND ASSOCIATED EQUIPMENT

The primary test apparatus used in this work consists of a stainless steel/glass/plexiglass vacuum chamber, two roughing pumps, a turbomolecular vacuum pump, an Argon supply system, high voltage DC power supply, and various metering equipment such as a volt meter, ammeter and oscilloscope. The vacuum chamber is a cylindrically shaped glass chamber with a removable plexiglass top cover, and a bottom stainless steel interface where a high-vacuum gate valve connects to the turbomolecular vacuum pump. The stainless steel interface also has various ports to connect the two roughing pumps, the Argon supply system and the various electrical leads from/to the power supply and metering equipment. One of the roughing pumps is mounted to the side of the turbo pump and is used to draw the pressure of the chamber down to the tens of milli-Torr range before the turbo pump is started. The thesis written by Frank Perry covers the vacuum chamber set up in more detail [7]. For start up sequence and operation procedures refer to Appendix A.

Once the Turbo molecular pump is engaged and draws the vacuum down to the range of 10^{-6} Torr the turbo pump and roughing pump are isolated and Argon is back filled into the chamber to the desired pressure for testing by the use of a metering valve. The pressure in the chamber is monitored by thermocouple sensors and a filament sensor.

A DC power supply is used to feed voltage to the sample wafer in the chamber while the breakdown voltage is monitored by and oscilloscope and a voltmeter with an ammmeter to measure the current drawn.

Once the breakdown voltage has been achieved the system is reset for the next experiment by evacuating the chamber to 10^{-6} torr.

B. MICRO-STRUCTURED ELECTRODE ARRAY WAFERS

The MSE structures used in these experiments are made from two copper layers sandwiching a fiberglass laminate epoxy resin system combined with a glass fabric substrate insulator. These Cu-dielectric-Cu structures are cut from larger sheets into approximately two inch by two inch pieces. These are then marked appropriately for

insulator thickness and nine micro-holes are drilled, using a precision drill press, in the center in a three by three grid pattern. The holes are spaced so that they are 2 mm apart. Each wafer is then etched using Ferric Chloride so as to strip the copper away from the edges – thus leaving 10 mm of dielectric exposed to prevent current flow across the edges [7].

Once etched, they are cleaned of oils and other contaminants by immersion into an alcohol bath and rubbed down. Excess alcohol is allowed to evaporate. Each wafer is then inspected for contaminants and then placed into the vacuum chamber for experimentation as needed [7].

III. THEORY OF IONIZATION ENGINE MODIFICATIONS

A. TOWNSEND THEORY OF BREAKDOWN

The concept behind the use of MSE arrays is to enhance the local electric field when a potential difference is applied to the electrodes. Within a gaseous medium such as Argon, the high field regions free electrons that can be amplified in an avalanche process. When the electric field exceeds a threshold level the number of charged particles multiplies exponentially and a discharge is started [6].

When a sufficiently strong electric field is applied, breakdown occurs. Breakdown is the process where a gas is converted from a non conducting material to a conducting one.

From the Townsend theory of breakdown, we know that the charge carriers are produced by volume processes. This is depicted by the ionization coefficient α, and by secondary emission coefficient γ. To start a self sustaining discharge, for every electron lost at the anode one has to be replaced by a secondary electron that was created in the gas or at the cathode. The ionization coefficient depicts how the electrons multiply in the gas medium in the direction of the electric field. The second ionization coefficient depicts the electron production at the cathode-gas interface. The secondary coefficient explains the effect of ions, photons, and neutrals [1].

At low pressures the production of electrons is primarily caused by ion impact on the cathode surface. The breakdown voltage can be shown in Equation (1) to be:

$$V_b = \frac{Bpd}{\ln(pd) + \ln\left(\frac{A}{\ln(1+\gamma^{-1})}\right)} \tag{1}$$

where p is the pressure of the gas medium in Torr (760 Torr = 1 atmosphere at sea level, 1 Torr = 133.289 N/m^2), d is the distance between parallel-plate anode and cathode in cm, A and B are constants that vary for each gas medium [1]. The breakdown voltage can be graphically represented by the use of a Paschen curve, which depicts the breakdown voltage versus pressure-times-distance as shown by plotting Equation 1 in

nondimensional form in Figure 2. This curve was generated using the general equation (Equation 2) for a Paschen curve.

$$Y = \frac{X}{\ln(X)} \tag{2}$$

Where Y represents the Breakdown voltage and X represents the pressure times distance. Figure 3 shows the general Paschen curve for an Argon medium.

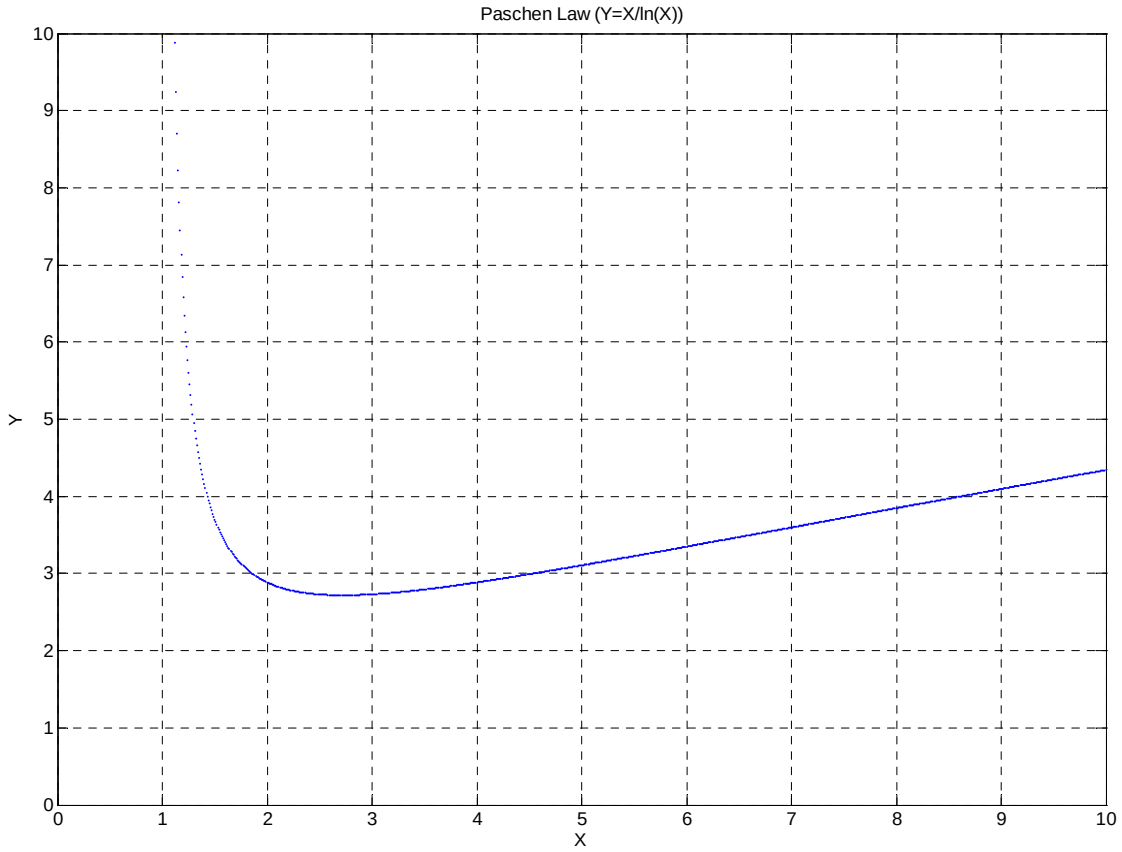

Figure 2. General Paschen Curve.

On the left hand side of a Paschen curve the breakdown voltage rises rapidly as pressure times distance (*pd*) decreases due to the low possibility of ionizing collisions requiring a strong electric field. On the right hand side of the curve the breakdown voltage rises gradually as *pd* increases due to the probability that an electron will produce ionization even at lower electric fields than the left hand side. The minimum of the curve is where the ionization process occurs at the minimum breakdown voltage. This

minimum voltage region is characterized by a specific *pd* and these two parameters are the primarily concerns for the miniaturization of the ionization chamber and are explored in detail throughout this thesis.

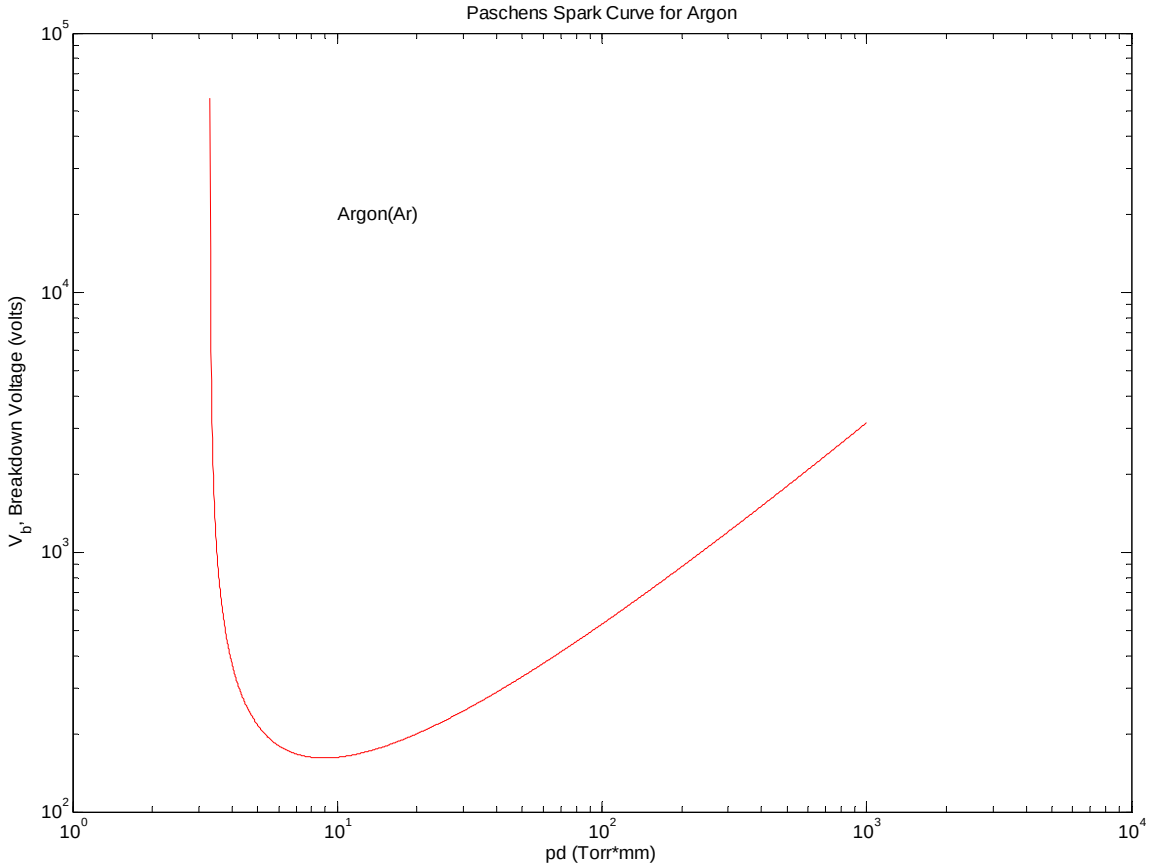

Figure 3. Argon Paschen Curve using a log scale.

The limitation of the Townsend theory is its assumption of homogeneous electric fields and *pd* values. When using non-homogeneous fields and variable geometry the Townsend theory breaks down and it is necessary to determine the field structure that is being produced. Experiments with the MSE geometries differ greatly form those with planar geometries discussed previously.

B. MSE ARRAY GEOMETRY

With three-dimensional MSE array geometries it can be expected that high electric fields can be achieved locally within the structure. The electric field structure in the MSE array can be expected to be non uniform with respect to planar geometries and

localized within the structure. Due to the imperfect manufacturing techniques used for these experiments the precise geometry of the individual holes differs slightly from each other. The high electric field thus generated in the structure is desirable for the ionization of Argon producing plasma and aids in electron emission from the cathode [6].

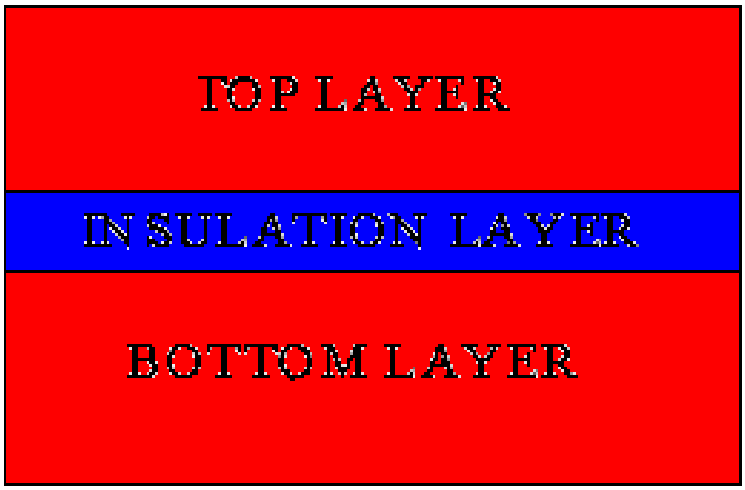

Figure 4. Cross-sectional view of Cu-dielectric-Cu layers without microhole structures.

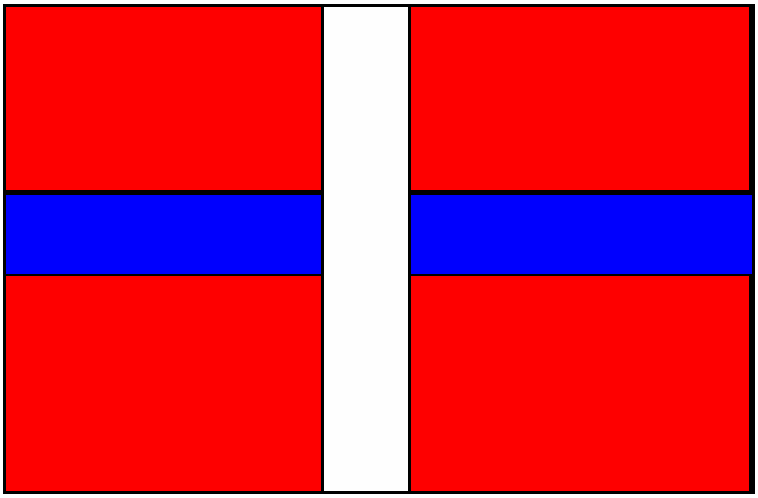

Figure 5. MSE array Cross-sectional view of Cu-dielectric-Cu layers with microhole structures (Hole diameters from 300 μm to 500 μm).

The three-dimensional MSE array geometry used is a three-by-three grid of holes in a two-inch by two-inch structure of two copper layers sandwiching a silicate insulator. The copper layers represent the electrodes. Figure 4 is a cross sectional representation of

this composite structure. Figure 5 is a cross sectional representation of the wafer with a hole drilled through it from top to bottom. Each of the nine holes can be a source of a micro-discharge that takes place between the two copper layers as they are in parallel. The insulation layers used for this experiment range in thickness from 100μm to 400μm and the holes range in diameter from 300μm to 500μm. For further information on the wafer construction please refer to Perry [7].

C. FIELD EMISSION

Field emission of electrons from the cathode could be a primary agent causing ionization in these experiments. Field emission is the process by which electrons are liberated from a surface that is under the effect of an electric field. These electrons are then accelerated in the applied electric field until they collide with neutral species, in the case of Argon gas these are atomic species. During the collision, additional electrons are liberated, which in turn are accelerated by the electric field and collide with other atoms ionizing them and producing even more electrons and so on causing an avalanche effect. This is an avalanche situation due to the exponential nature of the electron liberation.

Our experiments will benefit by utilizing the field emission effect to cause ionization in an Argon medium. The unique geometry of the three dimensional MSE arrays creates a concentrating effect of an applied electric field allowing the liberation of some electrons through the field emission effect at lower energy levels than would be required with parallel electrodes. There may be ways to further enhance their effects through manufacturing improvements and through the introduction of carbon nanotubes at the cathode [4].

THIS PAGE INTENTIONALLY LEFT BLANK

IV. EXPERIMENTAL RESULTS

A. INTRODUCTION

The objectives of our experiments were to measure the breakdown voltages at various pressures for the composite-structures of three different thicknesses and with three different diameter holes. (See Table 1.) The thickness refers to the thickness of the insulation between the copper layers for each composite structure on Figure 3. There were a total of twelve structures utilized in the experiments not including a few that were used to determine appropriate equipment set up. The twelve structures were organized into three groups of four. Each group consisted of a baseline structure without holes that was used to determine a baseline breakdown voltage for the operating pressures used. The other three consisted of one wafer each with 300, 400, 500μm diameter holes respectively.

Group one 127 μm structure	Group two 254 μm structure	Group three 381 μm structure
Baseline	Baseline	Baseline
300μm holes	300μm holes	300μm holes
400μm holes	400μm holes	400μm holes
500μm holes	500μm holes	500μm holes

Table 1. Composite Structure's Experimental Matrix.

Each MSE was attached to leads from the high voltage DC power supply and placed inside the vacuum chamber which was subsequently evacuated to a minimum of 10^{-6} Torr and then back filled with ultra pure research grade Argon (with a purity of 99.995%) to the needed experimental pressures. After each measurement the vacuum chamber was once again evacuated to remove ionized Argon and any contaminants and then backfilled with Argon to the next pressure. The breakdown voltage was determined by increasing the applied voltage and monitoring the voltage with a Tektronix oscilloscope. Once breakdown voltage was achieved the voltage level was recorded. (See Appendix A for diagrams of equipment and operational procedures.)

Once the breakdown voltages were obtained for all microstructures the data was put into MATLAB and graphed. (See appendix B for data tables of breakdown voltages and Paschen curves.) A typical Paschen curve for Argon is given in Figure 3. The data was then analyzed to determine where the minimum breakdown voltage occurred for each test case.

B. CALCULATING EXPECTED RESULTS

Once the experimental data was obtained, it was compared with the expected results. To determine the expected results a Paschen curve was generated for each structure. The expected Paschen curves were found by determining the experimental constants using Equation (3):

$$V_b = \frac{C_1 * pd}{\ln(pd) + \ln(C_2)} \tag{3}$$

where C_1 and C_2 are the experimental constants and V_b the breakdown voltage. Solving for the minimums using Equations (4) and (5) gives:

$$pd_{\min} = \frac{2.718}{C_2} \tag{4}$$

$$V_{b\min} = \frac{2.718 * C_1}{C_2} \tag{5}$$

where pd_{min} and $V_{b\ min}$ are the minimum values from the experimental data. The following three tables (Tables 2, 3, 4) show the MATLAB calculated C_1 and C_2 values for each micro structure:

Group 1 C_1 & C_2 Values		
Hole Diameter	C_1 (Volts^{-1})	C_2 (Torr^{-1}-cm^{-1})
Baseline	181820.00	1764.90
300µm	172910.00	1926.20
400µm	107800.00	1153.60
500µm	164040.00	1741.60

Table 2. Group 1 C_1 & C_2 MATLAB calculated values.

Group 2 C_1 & C_2 Values		
Hole Diameter	C_1 (Volts^{-1})	C_2 (Torr^{-1}-cm^{-1})
Baseline	71994.00	627.1777
300µm	101420.00	1111.6000
400µm	92142.00	894.4320
500µm	95202.00	1035.0000

Table 3. Group 2 C_1 & C_2 MATLAB calculated values.

Group 3 C_1 & C_2 Values		
Diameter	C_1 (Volts^{-1})	C_2 (Torr^{-1}-cm^{-1})
Baseline	50690.00	488.5677
300µm	60938.00	707.8125
400µm	92879.00	934.9845
500µm	38286.00	369.0127

Table 4. Group 3 C_1 & C_2 MATLAB calculated values.

Interesting to note is the C_1 and C_2 values decrease as the thickness of the wafers increases. The values also decrease as the hole diameter decreases.

The next step was to graph the expected Paschen curve and compare it to the curve generated by the experimental data.

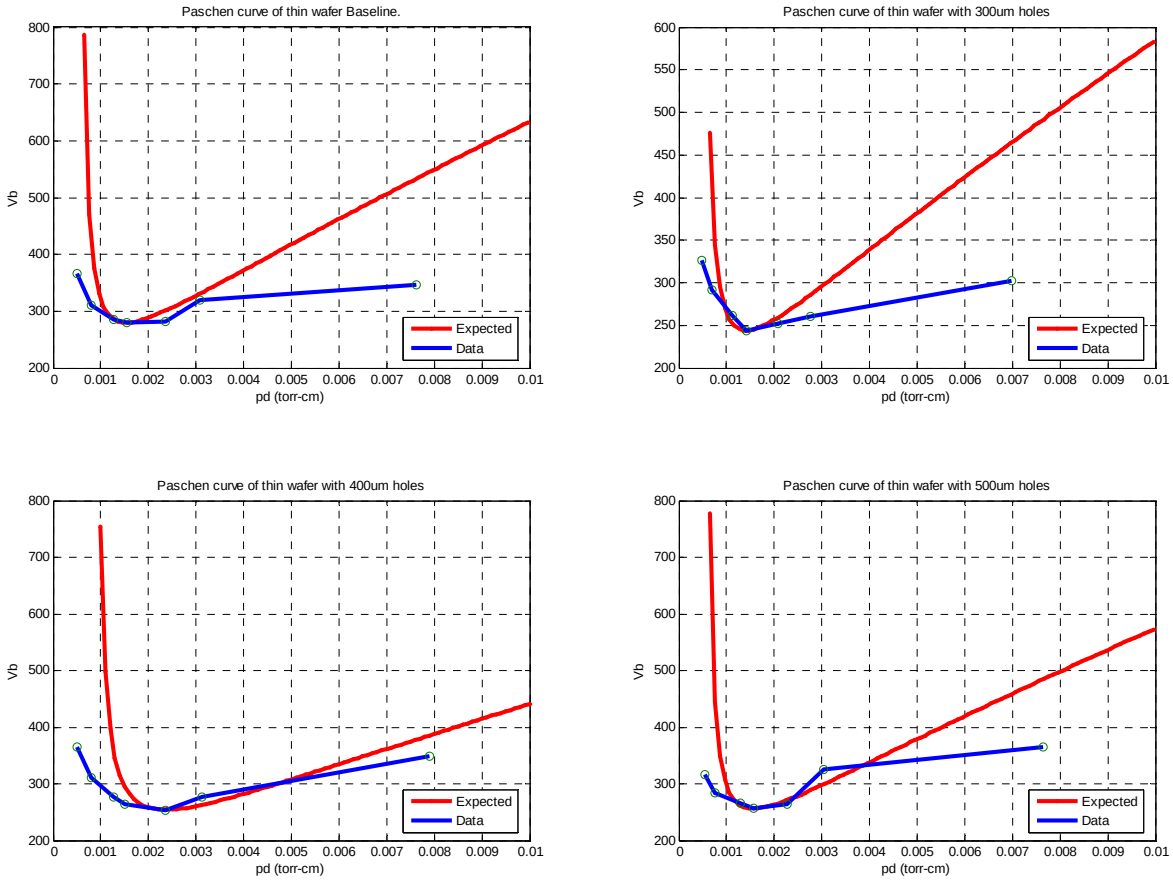

Figure 6. Graphical Representation of group one (thin) wafer actual breakdown voltages and expected breakdown voltage curve.

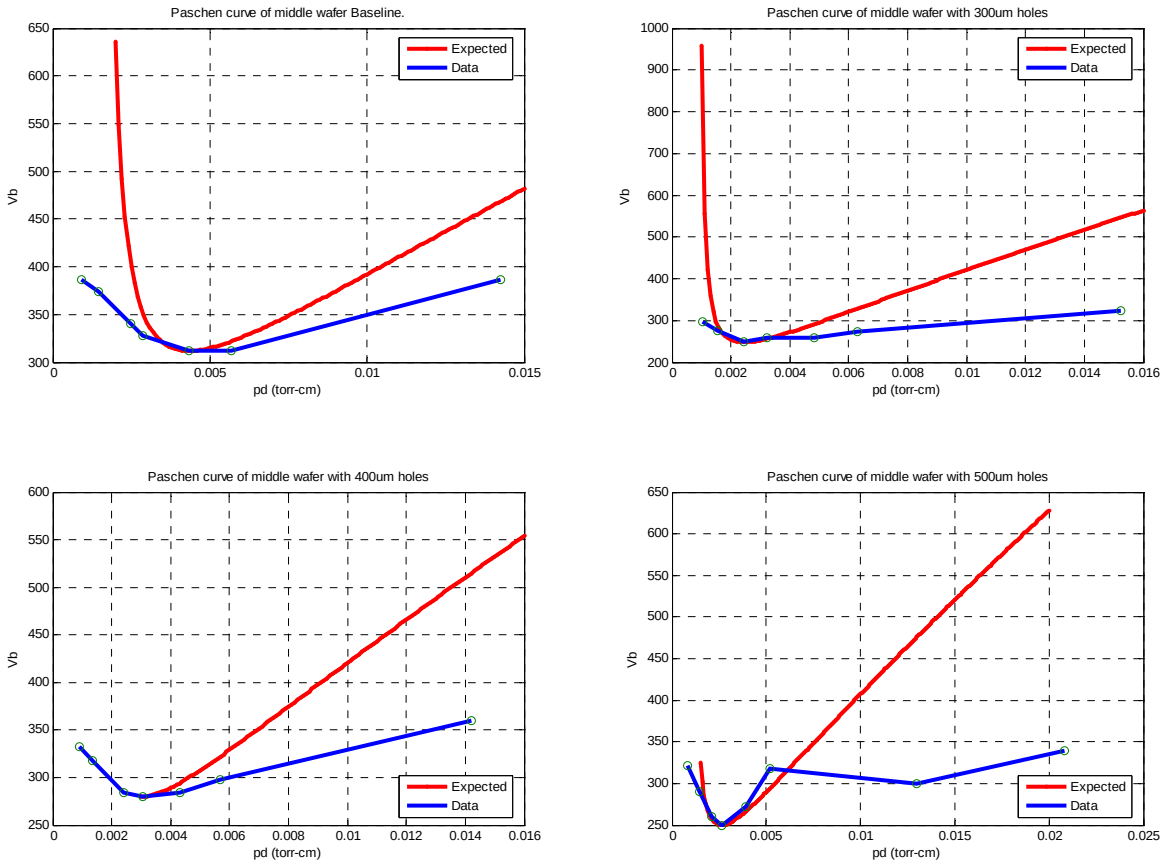

Figure 7. Graphical Representation of group two (middle) wafer actual breakdown voltages and expected breakdown voltage curve.

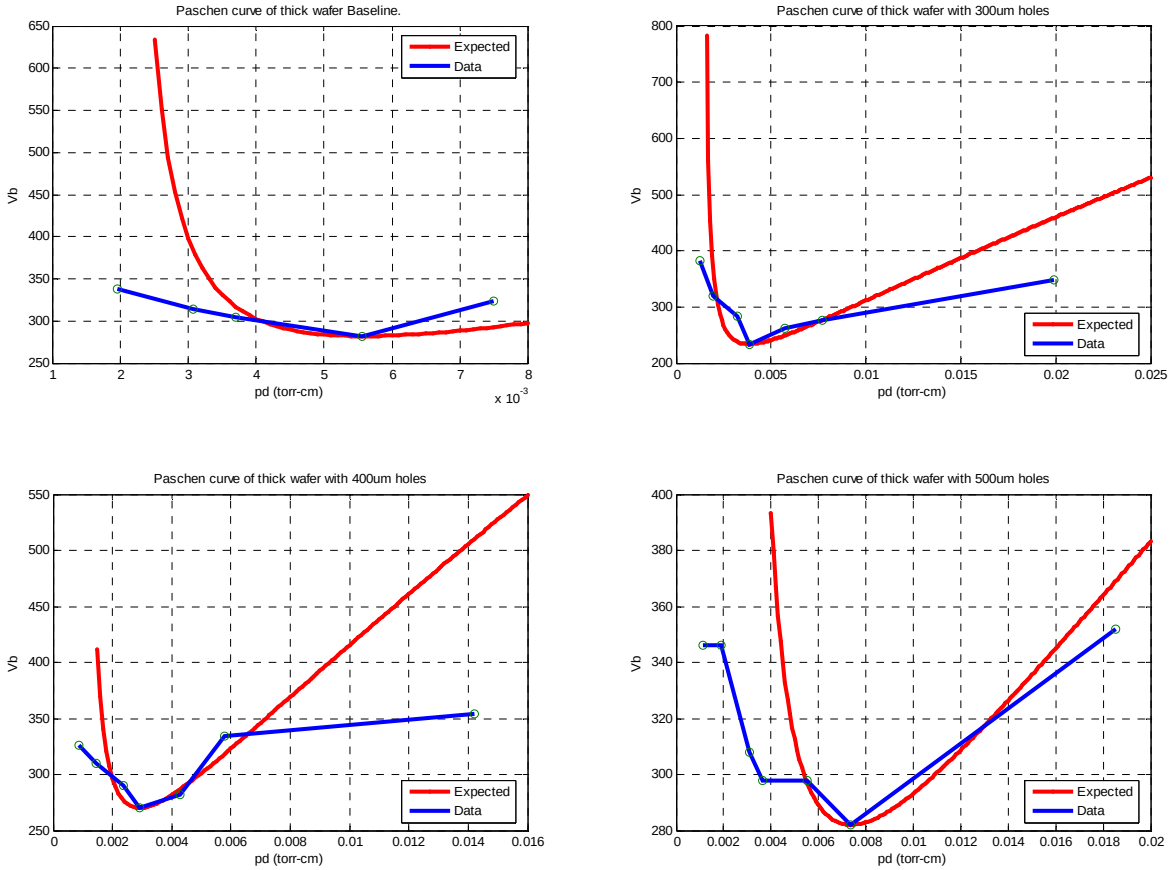

Figure 8. Graphical Representation of group three (thick) wafer actual breakdown voltages and expected breakdown voltage curve.

As can be seen in Figures 6, 7 and 8, the lowermost data points are close to the expected curves. Some variation can be seen but the minima are very close.

C. REPEATABILITY

The next question to be answered was whether the experiments can be duplicated with some degree of consistency. Two wafers were randomly chosen to be retested with the following results (Tables 5 and 6, Figures 9 and 10):

400µm – Group 2 structure with d=0.285mm/0.0112in			
First Run		Second Run	
Pressure (p) (milli-Torr)	Breakdown Voltage (Volts)	Pressure (p) (milli-Torr)	Breakdown Voltage (Volts)
11.2	N/A	N/A	N/A
30.3	326	30	318
51.3	310	50.7	292
83.7	290	80.9	268
102	270	101	248
150	282	150	292
203	334	200	316
498	354	499	288

Table 5. Data table contrasting the first and second run with the same wafer.

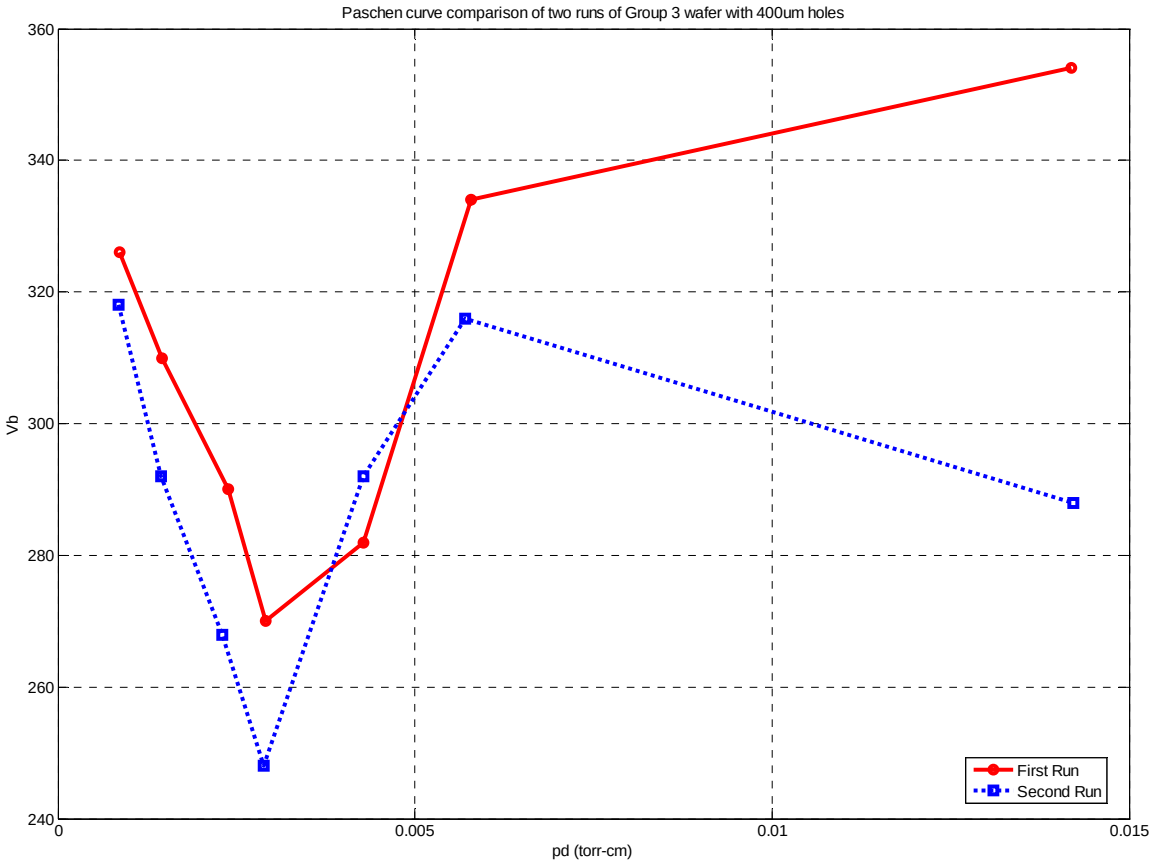

Figure 9. Comparison of Paschen curves for two runs of the middle wafer with 400µm diameter holes.

The comparison between the first and second runs (as shown in figure 9) of the middle wafer with 400µm diameter holes shows a high degree of similarity. The minimum voltages are within 22 volts of each other at the same pressure.

500µm – Group 3 structure with d=0.372mm/0.01465in			
First Run		Second Run	
Pressure (p) (milli-Torr)	Breakdown Voltage (Volts)	Pressure (p) (milli-Torr)	Breakdown Voltage (Volts)
10.6	N/A	N/A	N/A
30.7	346	34	316
50.6	346	50	306
83.1	308	81.6	292
98.2	298	N/A	N/A
149	298	150	296
198	282	201	306
498	352	N/A	N/A

Table 6. Data table contrasting the first and second run with the same wafer

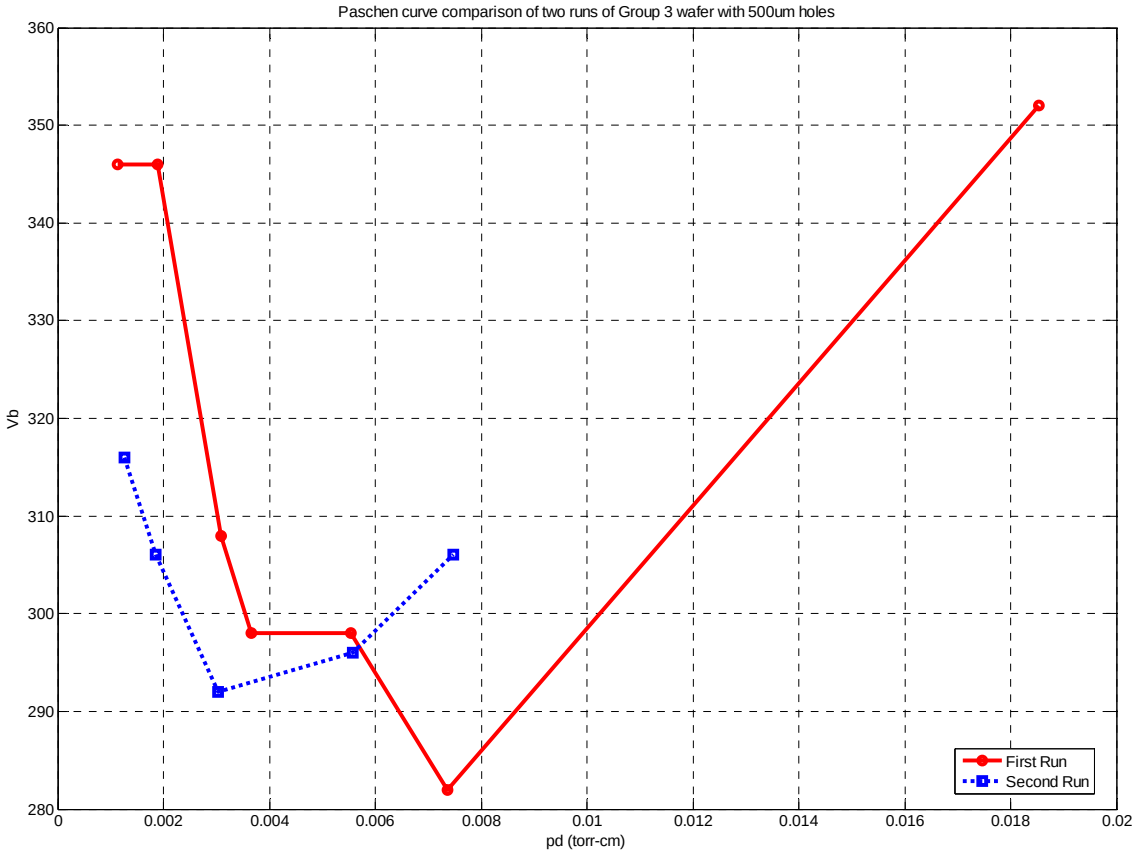

Figure 10. Comparison of Paschen curves for two runs of the thick wafer with 500µm diameter holes

The comparison of the first and second runs (as shown in Figure 10) of the thick wafer with 500µm diameter holes shows that there is less consistency between these runs.

The minimum voltage for breakdown varies by 10 volts but the pressure regions vary by 116 Torr with the first run minima occurring at 198 Torr and the second run minima occurring at 81.6 Torr.

The difference between the two runs can be in part contributed to the wear on the electrodes of the microstructures, which modifies the three dimensional geometry slightly.

D. DETERIORATION

One of the main unknowns of this experiment is the amount of deterioration of the electrodes during the ionization process. The purpose of this experiment is not to quantify the amount of deterioration of the electrodes but it must be realized that the deterioration will change the three dimensionality of the geometry over time. The deterioration is a function of the time that the electrodes are under discharge conditions; the robustness of the material used for the electrodes; and the voltage-current conditions. In our case copper was used to demonstrate that deterioration did in fact take place on the MSE arrays that were examined both before and after the ionization process. Microscope images are presented below –please see Perry [7] for further details.

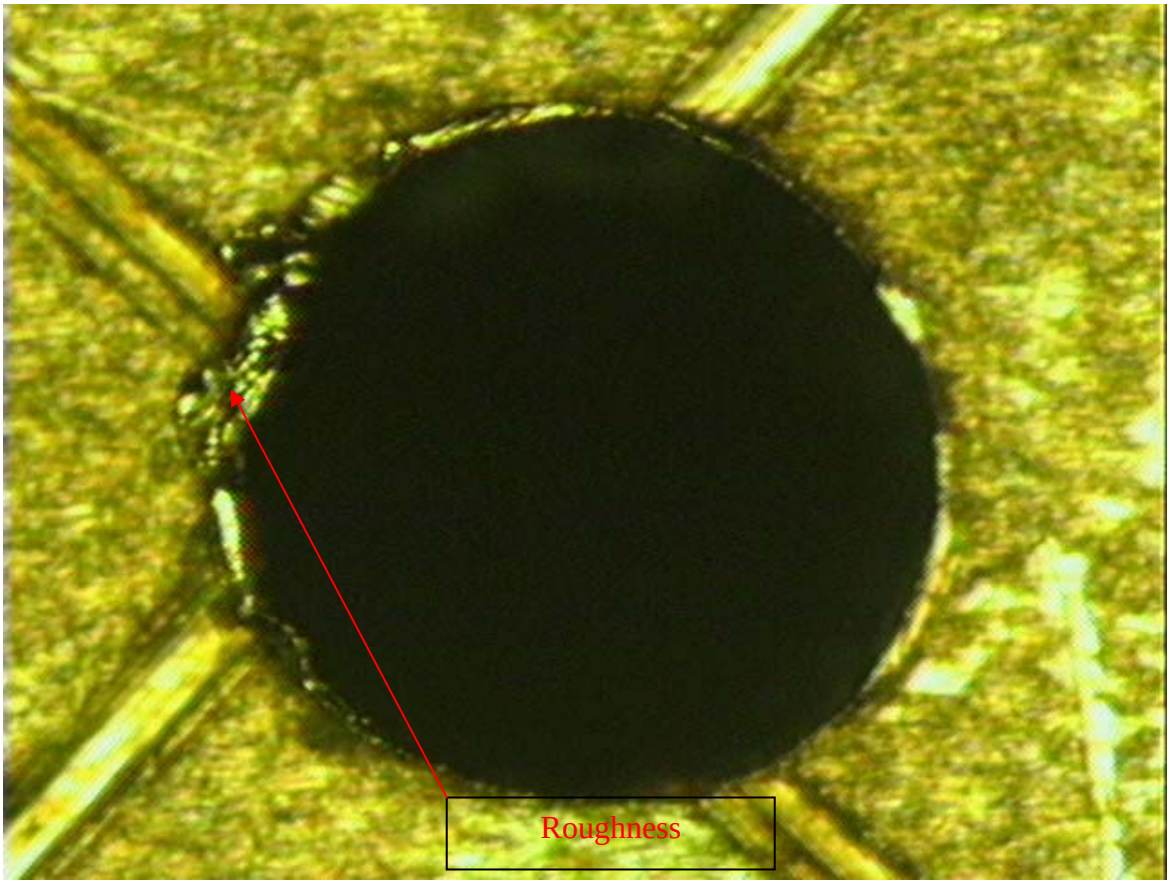

Figure 11. Photo of 300µm diameter hole at 290 magnification before testing.

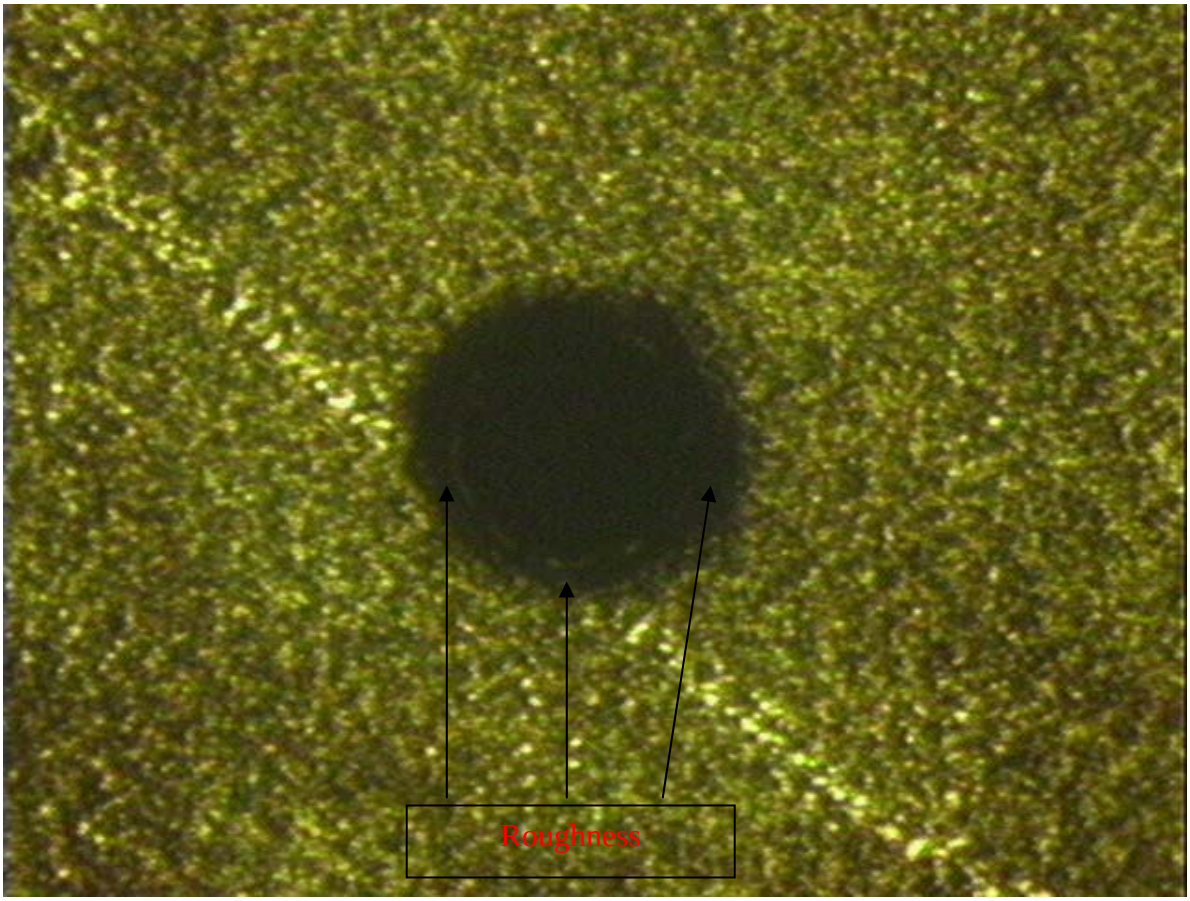

Figure 12. Photo of 400µm diameter hole at 48 magnification before testing.

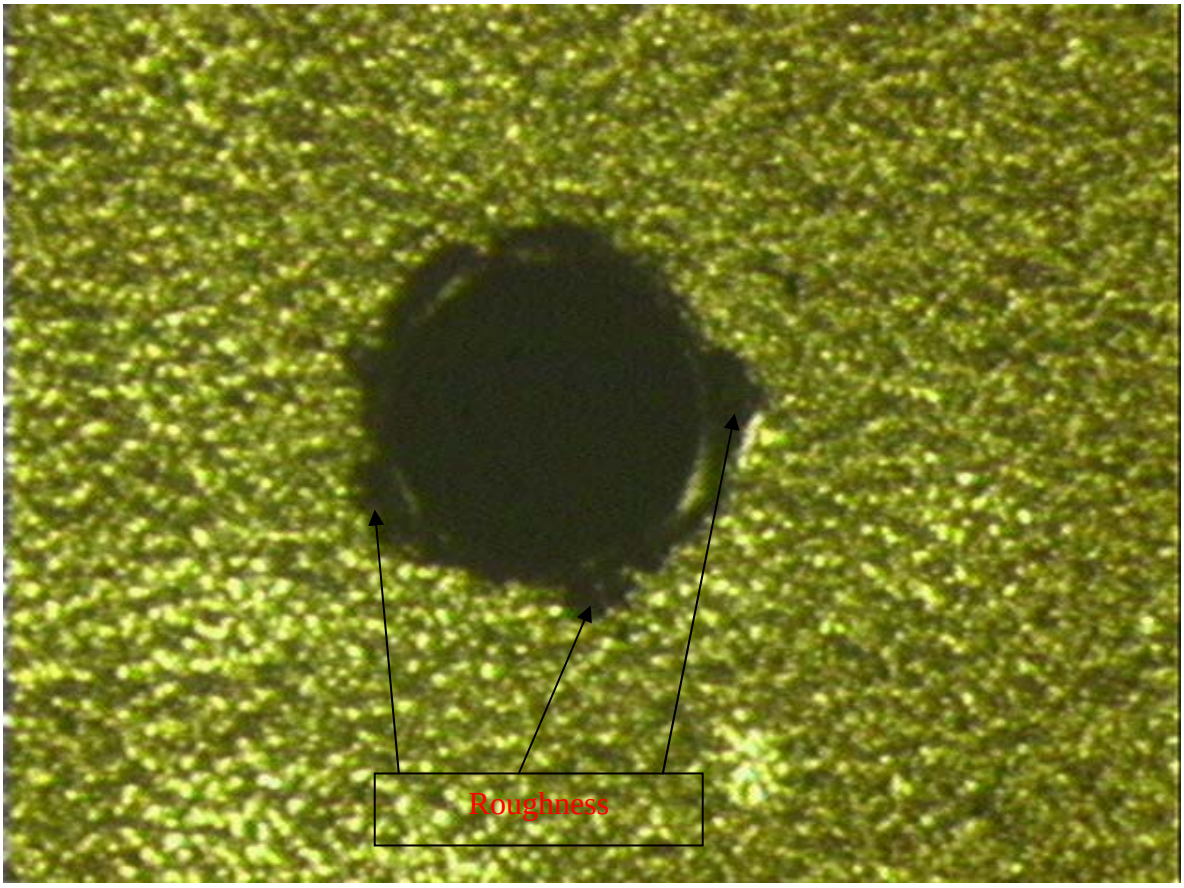

Figure 13. Photo of 500µm diameter hole at 48 magnification before testing

In Figures 11, 12 and 13 some roughness around the edges of the hole can be seen but these are due to the inaccuracies of the manufacturing methods used.

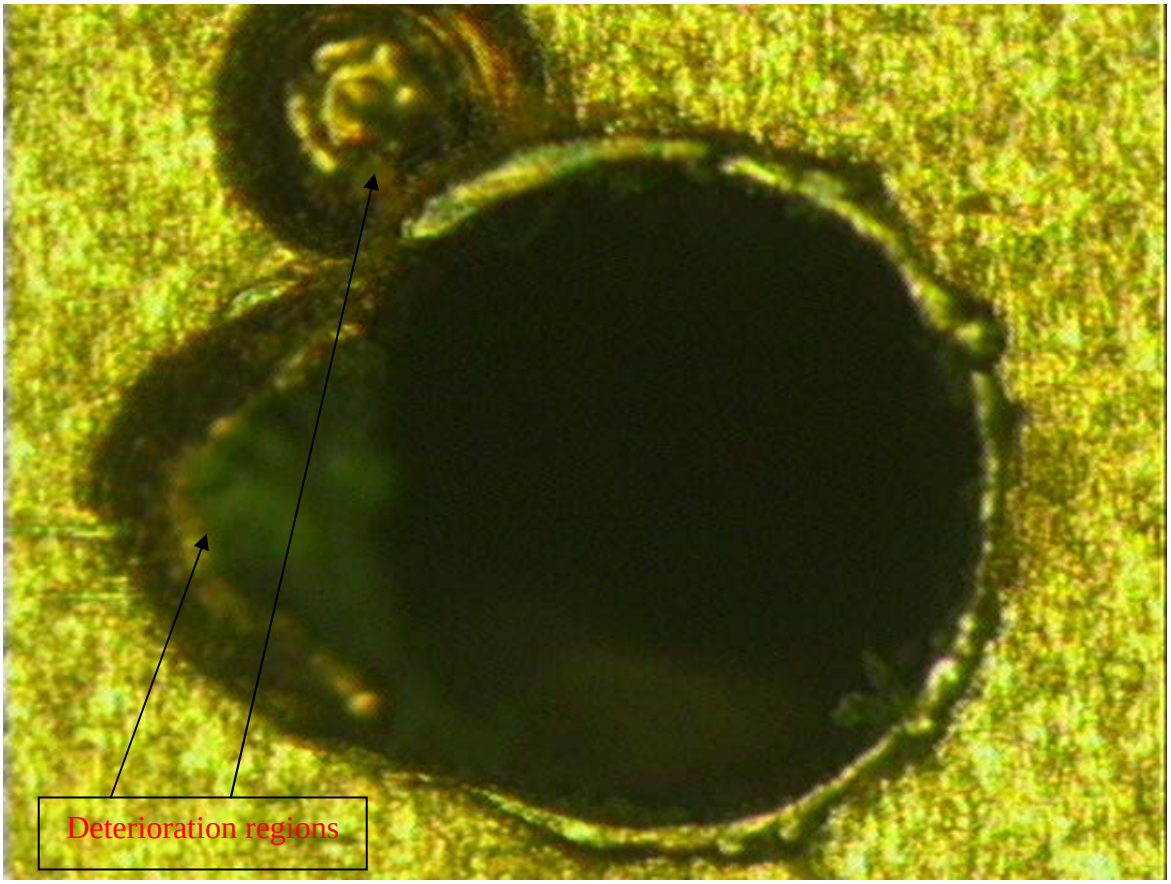

Figure 14. Photo of 300μm diameter hole at 290 magnification after testing.

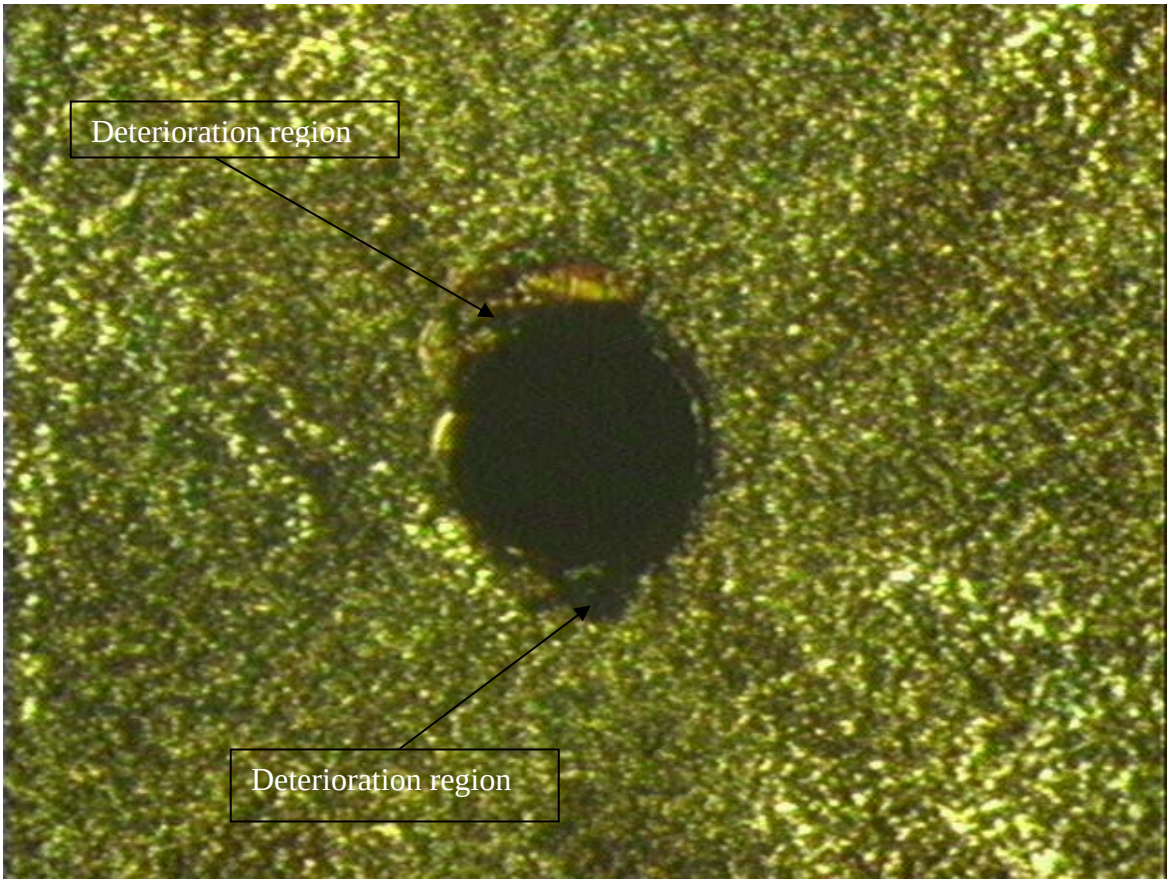

Figure 15. Photo of 400µm diameter hole at 48 magnification after testing.

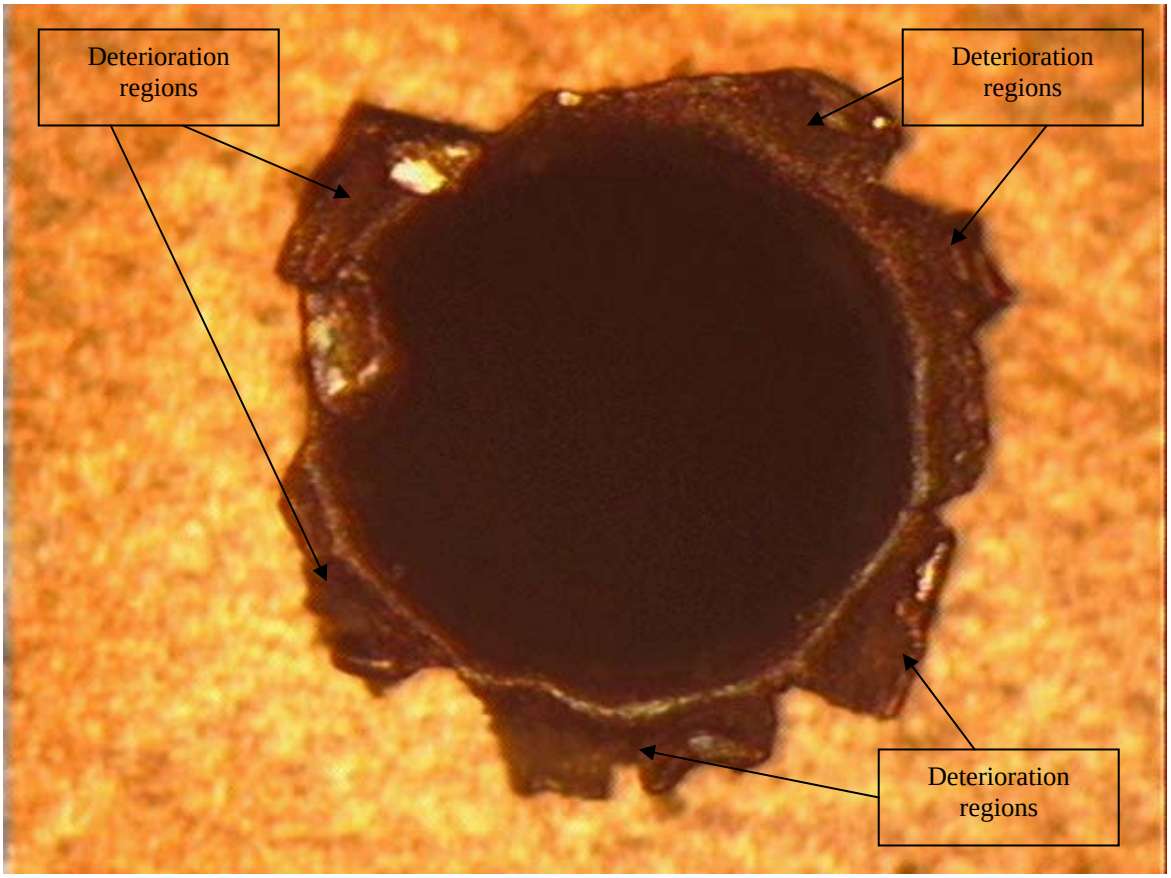

Figure 16. Photo of 500μm diameter hole at 290 magnification after testing

As can be seen in Figures 14, 15 and 16, there is significant deterioration of the electrodes after the ionization process in Argon has occurred. The amount of deterioration varies depending on the hole size and the time that the hole was subjected to the discharge. In this respect, copper was not a robust electrode material – ion engines require long life times, therefore future research must include the study of suitable electrode materials.

THIS PAGE INTENTIONALLY LEFT BLANK

V. CONCLUSIONS

This thesis shows that the ionization of Argon, which is an alternate fuel to Xenon, can be achieved at low voltages by utilizing Micro-Structured Electrode (MSE) arrays. The MSE arrays serve to concentrate the electric fields between electrodes allowing the production of electrons enhancing the field emission effect. Minimum breakdown voltages between 240 and 280 volts at pressures of around 100 milli-Torr ($0.133 N/m^2$) were consistently obtained with arrays of hole diameter ranging from 300 to 500μm. The MSE arrays were fabricated from composite Cu-SiO2-Cu structures with varying thicknesses from 100 μm to 400 μm. The micro structures (holes) were fabricated using precision conventional machining and hole diameters between 300 and 500 um were achieved.

Using the experimental data and MATLAB we were able to obtain the experimental constants (C_1 and C_2) for the Paschen curves. With these values in hand the minimum breakdown voltages were calculated for each of the MSE arrays. The values of the experimental constants decreased as the thickness of the layered structures increased and as the hole diameter decreased.

Another achievement has been the utilization of commonly available materials and manufacturing methods for the construction of the MSE arrays. Thus yielding a low–cost method for conducting experiments in this field

THIS PAGE INTENTIONALLY LEFT BLANK

VI. RECOMMENDATIONS

Several recommendations resulted from this study

A. REPEATABILITY STUDIES

Additional repeatability studies should be performed to verify that ionization can be achieved for the same MSE array many times at the same voltage. This will also serve to establish accurate empirical data required for any future optimization studies.

B. DETERIORATION STUDIES

Further work should include the study of the rate and amount of deterioration that is incurred by repeating the ionization process many times with the same MSE array. With each repetition the three dimensionality of the structures changed and the modeling and understanding of this change will be vital to predicting future performance.

C. FLOW STUDIES

This experiment was conducted in a static atmosphere. Future ion engine applications will not be utilizing such an atmosphere but will instead be utilizing the flow of Argon through the MSE array. Additional studies should be performed to determine the effects of a flow (both constant and variable) through the array on the breakdown voltages and on ionization efficiency.

D. MATERIAL STUDIES

Another point of interest is the materials that make up the MSE array. For these experiments copper electrodes were used. Ion propulsion applications will require long life times, therefore suitable materials need to be identified

E. STRUCTURES STUDIES

The current experiment used a circular hole through the electrodes and insulator material. Other three dimensional structures should be investigated for optimal ionization performance and efficiency.

THIS PAGE INTENTIONALLY LEFT BLANK

APPENDIX A

A. PROCEDURE FOR VACUUM CHAMBER OPERATION.

Steps:

1. Vent vacuum chamber to normal atmospheric pressure by opening venting valve.
2. Open vacuum chamber and connect wafer to copper leads utilizing plastic clips. Ensure that the two copper leads are attached on opposite sides of the wafer from each other.
3. Close vacuum chamber and inspect seals. Ensure venting valve and roughing pump number 2 valve are closed. Open isolation valve and start roughing pump number 1.
4. Turn on instrument panel and thermocouple (TC) gages 1 and 2 and 3. Once TC2 and TC3 indicate chamber pressure around 100milli-Torr turn power on to the Turbo Molecular Pump (TMP) and monitor as power up sequence commences. Turn on Filament gage and monitor pressure.
5. Once vacuum chamber pressure is at its minimum pressure (approximately $1.5x10^{-6}$ Torr) fasten Argon line to vent valve on chamber and ensure metering valve is closed. Open pressure valve on Argon tank and open cut off valve to metering valve on Argon line to vacuum chamber.
6. Close Isolation Valve and begin backfilling vacuum chamber with Argon by opening vent valve and open metering valve. Adjust and control flow of Argon into Vacuum chamber by adjusting metering valve and monitoring TC3 meter.
7. Once pressure in vacuum chamber has reached required pressure shut off metering valve and close vent valve.

B. PROCEDURE FOR INSTRUMENT PANEL OPERATION

Steps:

1. Once the procedures in part A are complete and the experiment is ready to be run, turn on power to the equipment cabinet ensuring that the voltmeter, amp meter and oscilloscope power up.
2. Switch amp meter from AC to DC setting. Volt meter should default to DC setting. Set oscilloscope to 5 volts per division and 5 seconds per division.
3. For Safety Ensure No One is touching any wires or the vacuum chamber.
4. Ensure power supply is set to zero volts and turn on power supply.
5. Begin by incrementing voltage levels and monitor oscilloscope and voltmeter for breakdown voltage.
6. Once breakdown voltage has been achieved record voltage and turn off power supply and set dials on power supply back to zero volts.
7. Set up for next experiment.

C. DIAGRAMS

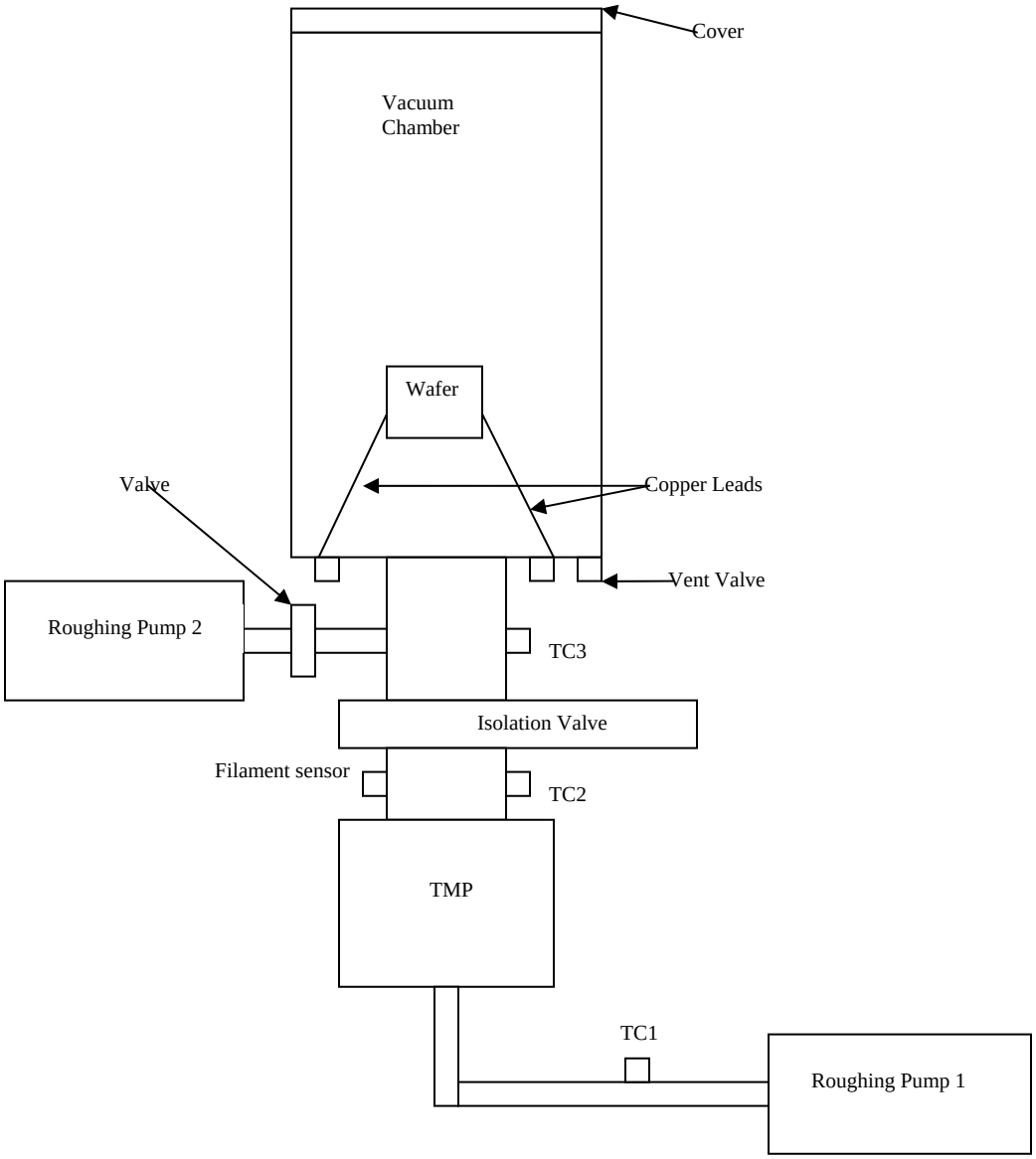

Figure 17. Diagram of vacuum chamber assembly.

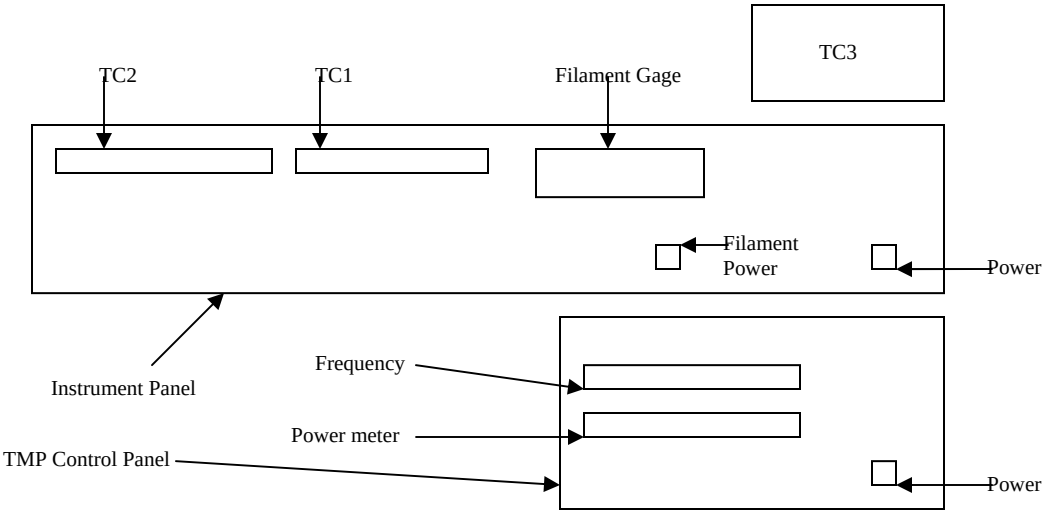

Figure 18. Diagram of control panel for pressure sensors and pump controls.

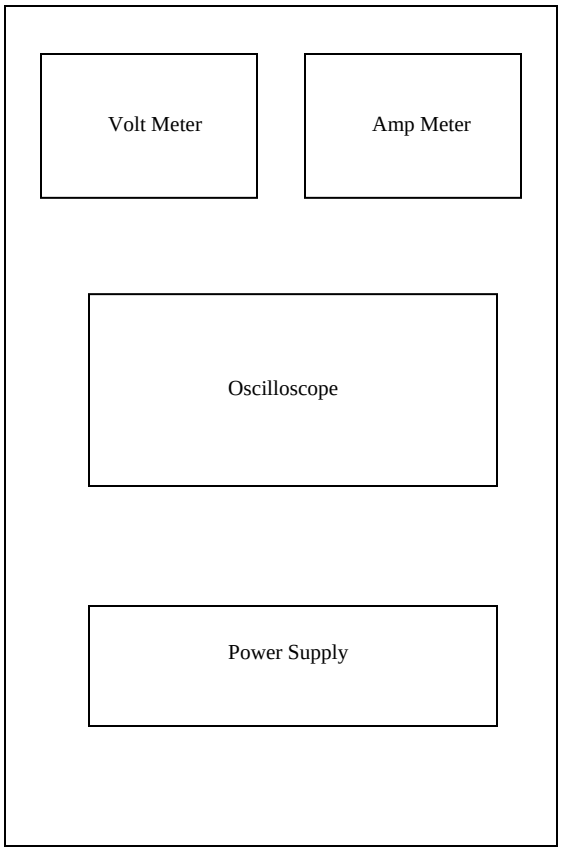

Figure 19. Layout of equipment rack.

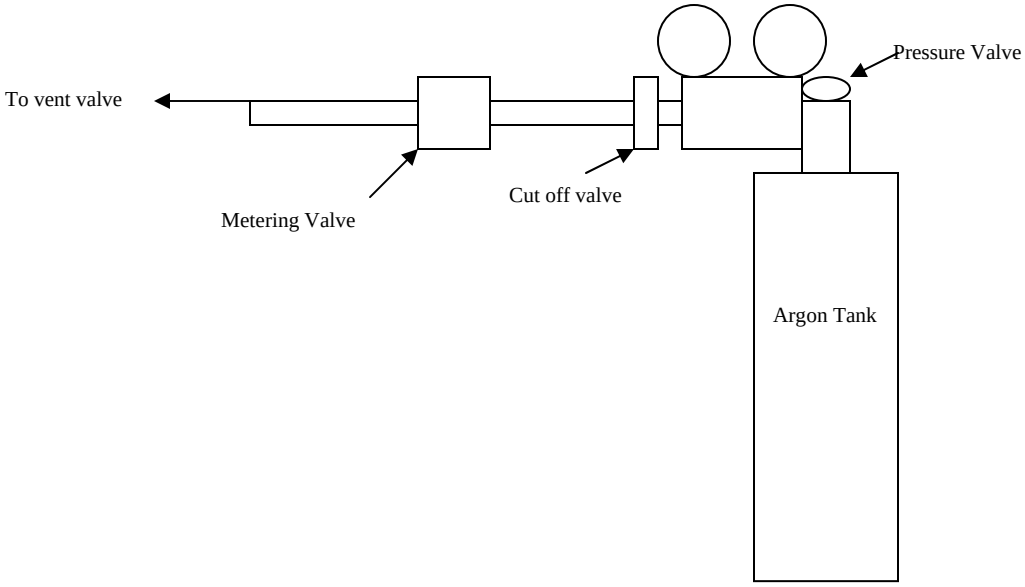

Figure 20. Argon supply system layout.

APPENDIX B

A. DATA TABLES

1. Group 1

Baseline - Thin Wafer with d=0.154mm/0.00605in	
Pressure (p) (milli-Torr)	Breakdown Voltage (Volts)
13.5	N/A
32.4	366
51.4	310
82.3	286
100	280
153	282
200	320
495	346

Table 7. Group 1 baseline.

300µm - Thin Wafer with d=0.137mm/0.00535in	
Pressure (p) (milli-Torr)	Breakdown Voltage (Volts)
13.8	N/A
35.2	326
51.3	292
82.2	262
103	244
151	252
202	260
509	302

Table 8. Group 1 with 300µm holes.

400um - Thin Wafer with d=0.153mm/0.00605in	
Pressure (p) (milli-Torr)	Breakdown Voltage (Volts)
13.4	N/A
32.1	364
52.9	310
82.9	276
98.3	264
154	254
204	276
517	348

Table 9. Group 1 with 400µm holes.

500um - Thin Wafer with d=0.136mm/0.00535in	
Pressure (p) (milli-Torr)	Breakdown Voltage (Volts)
13	N/A
35.1	316
50	284
83.8	266
102	256
148	264
199	326
500	364

Table 10. Group 1 with 500µm holes.

2. Group 2

Baseline - Middle Wafer with d=0.287mm/0.0113in	
Pressure (p) (milli-Torr)	Breakdown Voltage (Volts)
12.9	N/A
31.5	386
50.4	374
85.9	340
100	328
151	312
198	312
496	386

Table 11. Group 2 baseline.

300µm - Middle Wafer with d=0.303mm/0.0119in	
Pressure (p) (milli-Torr)	Breakdown Voltage (Volts)
11.9	N/A
33.9	296
50.9	276
80.7	248
106	258
159	258
208	274
503	324

Table 12. Group 2 with 300µm holes.

400µm - Middle Wafer with d=0.284mm/0.01115in	
Pressure (p) (milli-Torr)	Breakdown Voltage (Volts)
10.4	N/A
31.8	332
48	318
84.3	284
107	280
152	284
200	298
500	360

Table 13. Group 2 with 400µm holes.

500µm - Middle Wafer with d=0.26mm/0.01025in	
Pressure (p) (milli-Torr)	Breakdown Voltage (Volts)
11.9	N/A
31.7	322
56.6	290
81.4	260
101	250
150	272
200	318
499	300
800	340

Table 14. Group 2 with 500µm holes.

3. Group 3

Baseline - Thick Wafer with d=0.366mm/0.0144in	
Pressure (p) (milli-Torr)	Breakdown Voltage (Volts)
10	N/A
32.4	N/A
53.4	338
83.8	314
101	304
152	282
205	324
497	N/A

Table 15. Group 3 baseline.

300µm - Thick Wafer with d=0.384mm/0.0151in	
Pressure (p) (milli-Torr)	Breakdown Voltage (Volts)
14.1	N/A
32.2	382
50.7	320
84.1	284
100	234
149	262
200	276
518	348

Table 16. Group 3 with 300µm holes.

400µm - Thick Wafer with d=0.285mm/0.0112in	
Pressure (p) (milli-Torr)	Breakdown Voltage (Volts)
11.2	N/A
30.3	326
51.3	310
83.7	290
102	270
150	282
203	334
498	354

Table 17. Group 3 with 400µm holes.

500µm - Thick Wafer with d=0.372mm/0.01465in	
Pressure (p) (milli-Torr)	Breakdown Voltage (Volts)
10.6	N/A
30.7	346
50.6	346
83.1	308
98.2	298
149	298
198	282
498	352

Table 18. Group 3 with 500µm holes.

B. PASCHEN CURVE RESULTS

1. Paschen Curve Comparison of Data

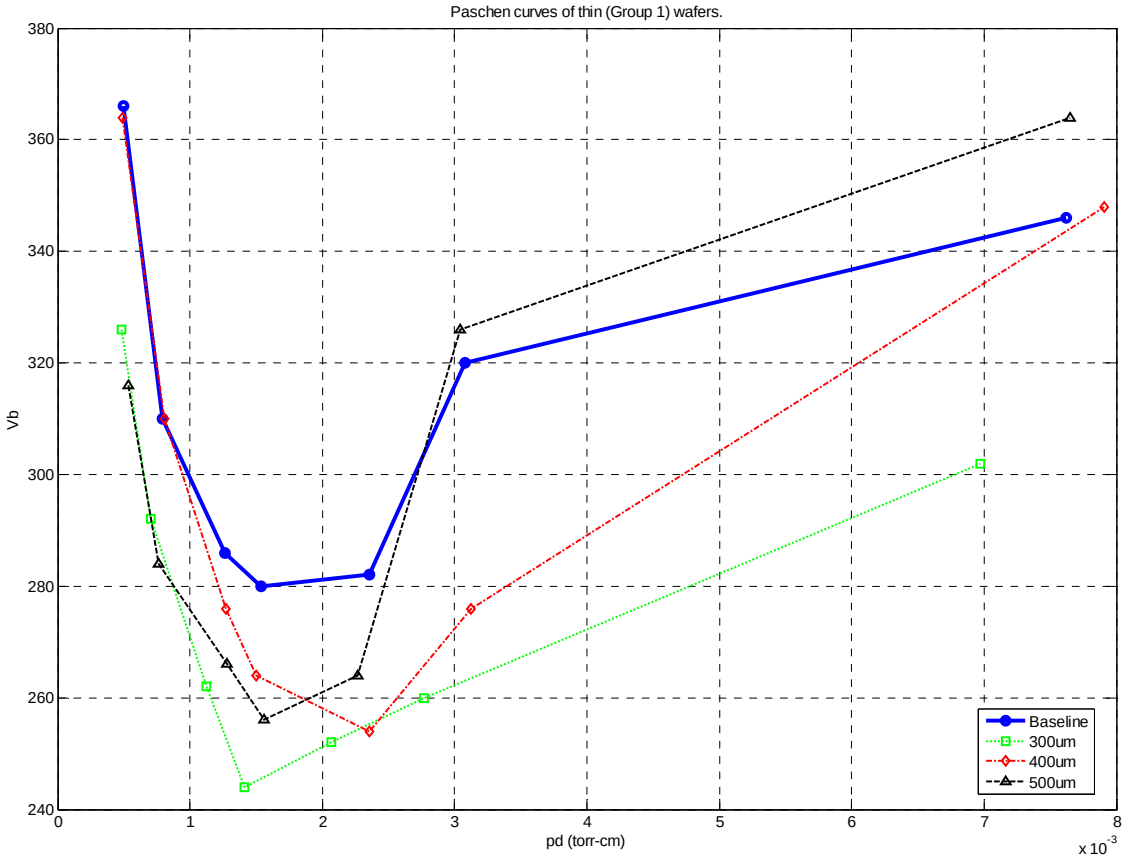

Figure 21. Comparison of thin (Group 1) breakdown voltages.

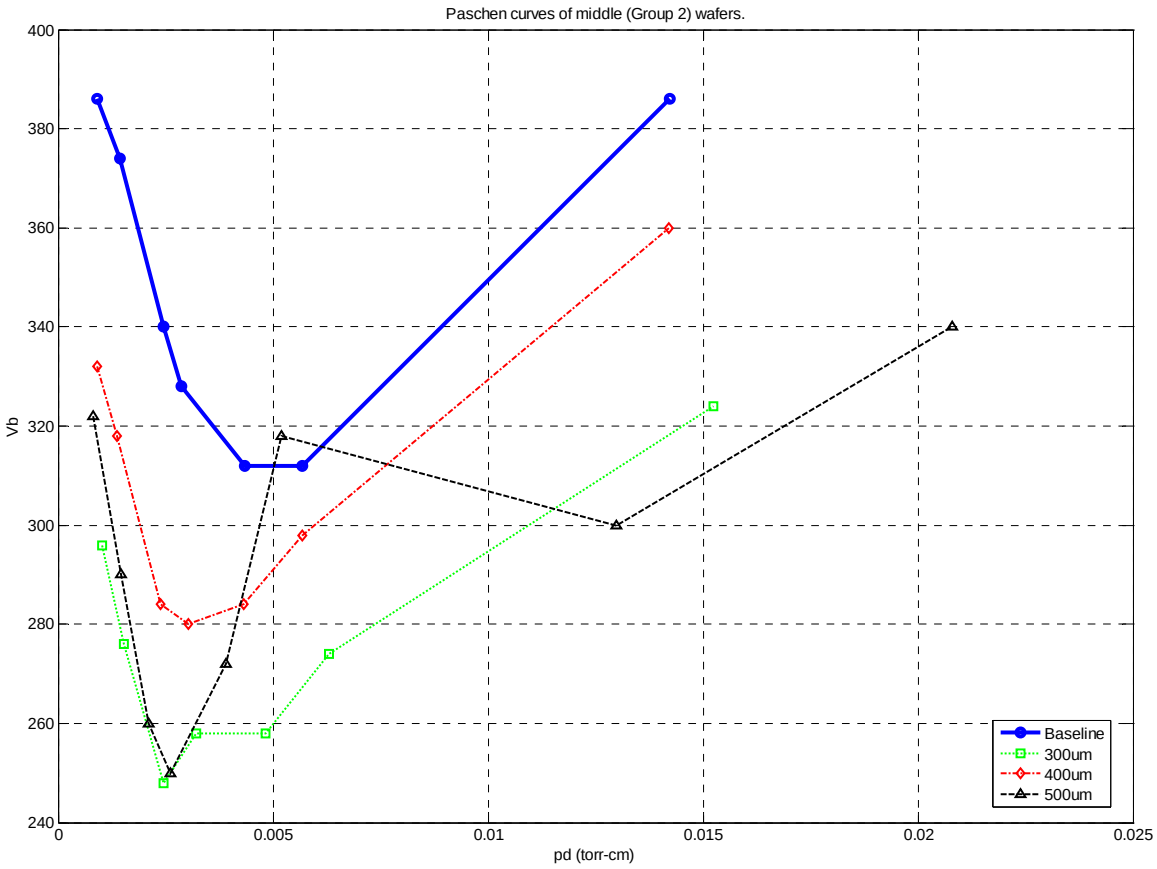

Figure 22. Comparison of middle (Group 2) breakdown voltages.

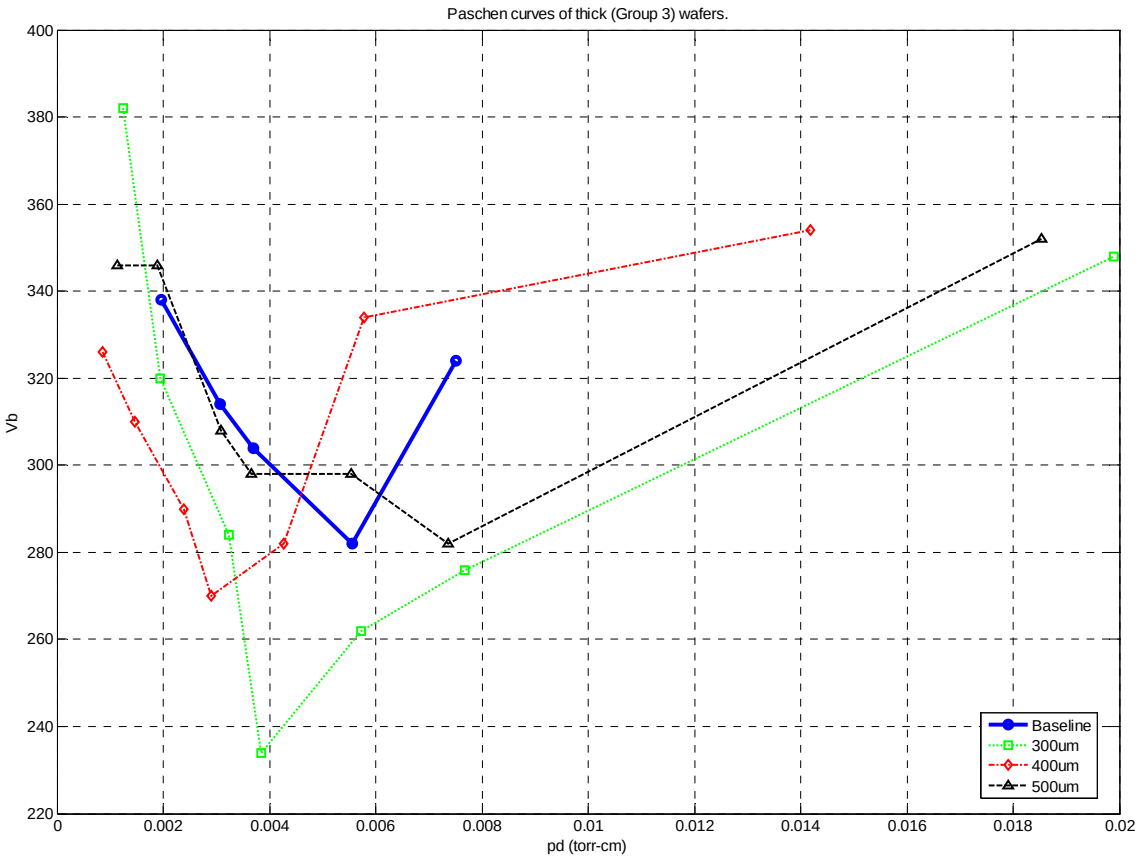

Figure 23. Comparison of thick (Group 3) breakdown voltages.

THIS PAGE INTENTIONALLY LEFT BLANK

APPENDIX C

A. MATLAB CODE USED TO GRAPH FIGURES 6-8

```
%% Thesis Data


clear all
close all
clc


%%%%Thinnest Wafers
%% Thinnest wafer Baseline
pdmin= 100*.0154  %milli-Torr
pdmin=pdmin/1000  %Torr
Vbmin=280
c2=2.718/pdmin
c1=Vbmin*c2/2.718
x=.00066:.0001:.01;
vb=(c1.*x)./(log(x)+log(c2));
figure(1)
subplot(2,2,1)
plot(x,vb,'r.-','linewidth',3)
hold on
d=.0154; %cm or 0.00605in
P=[32.4 51.4 82.3 100 153 200 495]; %% pressure in milliTorr
P=P/1000;  %% pressure in Torr
Vb=[366 310 286 280 282 320 346]; %% voltage in volts
pd=d*P;
plot(pd,Vb,'linewidth',3)
title('Paschen curve of thinnest wafer Baseline.')
xlabel('pd (Torr-cm)')
ylabel('Vb')
legend('Expected','Data','Location','SouthEast')
grid on
hold on
scatter(pd,Vb)
```

```
%% 300um thinnest wafer
pdmin= 103*.0137  %milliTorr
pdmin=pdmin/1000  %Torr
Vbmin=244
c2=2.718/pdmin
c1=Vbmin*c2/2.718
x=.00066:.0001:.01;
vb=(c1.*x)./(log(x)+log(c2));
subplot(2,2,2)
plot(x,vb,'r.-','linewidth',3)
hold on
d=.0137; %cm or 0.00535in
P=[35.2 51.3 82.2 103 151 202 509]; %% pressure in milliTorr
P=P/1000; %% pressute in Torr
Vb=[326 292 262 244 252 260 302]; %% voltage in volts
pd=d*P;
plot(pd,Vb,'linewidth',3)
title('Paschen curve of thinnest wafer with 300um holes')
xlabel('pd (Torr-cm)')
ylabel('Vb')
legend('Expected','Data','Location','SouthEast')
grid on
%axis tight
hold on
scatter(pd,Vb)

%% 400um thinnest wafer
pdmin= 154*.0153  %milliTorr
pdmin=pdmin/1000  %Torr
Vbmin=254
c2=2.718/pdmin
c1=Vbmin*c2/2.718
x=.001:.0001:.01;
vb=(c1.*x)./(log(x)+log(c2));
subplot(2,2,3)
plot(x,vb,'r.-','linewidth',3)
hold on
```

```
d=.0153; %cm or 0.00605in
P=[32.1 52.9 82.9 98.3 154 204 517]; %% pressure in milliTorr
P=P/1000; %% pressute in torr
Vb=[364 310 276 264 254 276 348]; %% voltage in volts
pd=d*P;
plot(pd,Vb,'linewidth',3)
title('Paschen curve of thinnest wafer with 400um holes')
xlabel('pd (torr-cm)')
ylabel('Vb')
legend('Expected','Data','Location','SouthEast')
grid on
hold on
scatter(pd,Vb)

%% 500um thinnest wafer
pdmin= 102*.0153  %millitorr
pdmin=pdmin/1000  %torr
Vbmin=256
c2=2.718/pdmin
c1=Vbmin*c2/2.718
x=.00066:.0001:.01;
vb=(c1.*x)./(log(x)+log(c2));
subplot(2,2,4)
plot(x,vb,'r.-','linewidth',3)
hold on
d=.0153; %cm or 0.00605in
P=[35.1 50 83.8 102 148 199 500]; %% pressure in millitorr
P=P/1000; %% pressute in torr
Vb=[316 284 266 256 264 326 364]; %% voltage in volts
pd=d*P;
plot(pd,Vb,'linewidth',3)
title('Paschen curve of thinnest wafer with 500um holes')
xlabel('pd (torr-cm)')
ylabel('Vb')
legend('Expected','Data','Location','SouthEast')
grid on
hold on
```

```
scatter(pd,Vb)

%%%%Middle Wafers
%% Middle wafer Baseline
pdmin= 151*.0287  %millitorr
pdmin=pdmin/1000  %torr
Vbmin=312
c2=2.718/pdmin
c1=Vbmin*c2/2.718
x=.002:.0001:.015;
vb=(c1.*x)./(log(x)+log(c2));
figure(2)
subplot(2,2,1)
plot(x,vb,'r.-','linewidth',3)
hold on
d=.0287; %cm or 0.0113in
P=[31.5 50.4 85.9 100 151 198 496]; %% pressure in millitorr
P=P/1000;  %% pressute in torr
Vb=[386 374 340 328 312 312 386]; %% voltage in volts
pd=d*P;
plot(pd,Vb,'linewidth',3)
title('Paschen curve of middle wafer Baseline.')
xlabel('pd (torr-cm)')
ylabel('Vb')
legend('Expected','Data','Location','NorthEast')
grid on
hold on
scatter(pd,Vb)

%% 300um middle wafer
pdmin= 80.7*.0303  %millitorr
pdmin=pdmin/1000  %torr
Vbmin=248
c2=2.718/pdmin
c1=Vbmin*c2/2.718
x=.001:.0001:.016;
vb=(c1.*x)./(log(x)+log(c2));
```

```
subplot(2,2,2)
plot(x,vb,'r.-','linewidth',3)
hold on
d=.0303; %cm or 0.0119in
P=[33.9 50.9 80.7 106 159 208 503]; %% pressure in millitorr
P=P/1000; %% pressute in torr
Vb=[296 276 248 258 258 274 324]; %% voltage in volts
pd=d*P;
plot(pd,Vb,'linewidth',3)
title('Paschen curve of middle wafer with 300um holes')
xlabel('pd (torr-cm)')
ylabel('Vb')
legend('Expected','Data','Location','NorthEast')
grid on
hold on
scatter(pd,Vb)

%% 400um middle wafer
pdmin= 107*.0284  %millitorr
pdmin=pdmin/1000  %torr
Vbmin=280
c2=2.718/pdmin
c1=Vbmin*c2/2.718
x=.003:.0001:.016;
vb=(c1.*x)./(log(x)+log(c2));
subplot(2,2,3)
plot(x,vb,'r.-','linewidth',3)
hold on
d=.0284; %cm or 0.01115in
P=[31.8 48 84.3 107 152 200 500]; %% pressure in millitorr
P=P/1000; %% pressute in torr
Vb=[332 318 284 280 284 298 360]; %% voltage in volts
pd=d*P;
plot(pd,Vb,'linewidth',3)
title('Paschen curve of middle wafer with 400um holes')
xlabel('pd (torr-cm)')
ylabel('Vb')
```

```
legend('Expected','Data','Location','SouthEast')
grid on
hold on
scatter(pd,Vb)

%% 500um middle wafer
pdmin= 101*.026  %millitorr
pdmin=pdmin/1000  %torr
Vbmin=250
c2=2.718/pdmin
c1=Vbmin*c2/2.718
x=.0015:.0001:.02;
vb=(c1.*x)./(log(x)+log(c2));
subplot(2,2,4)
plot(x,vb,'r.-','linewidth',3)
hold on
d=.026; %cm or 0.01025in
P=[31.7 56.6 81.4 101 150 200 499 800]; %% pressure in millitorr
P=P/1000; %% pressute in torr
Vb=[322 290 260 250 272 318 300 340]; %% voltage in volts
pd=d*P;
plot(pd,Vb,'linewidth',3)
title('Paschen curve of middle wafer with 500um holes')
xlabel('pd (torr-cm)')
ylabel('Vb')
legend('Expected','Data','Location','SouthEast')
grid on
hold on
scatter(pd,Vb)

%%%%Thick Wafers
%% Thick wafer Baseline
pdmin= 152*.0366  %millitorr
pdmin=pdmin/1000  %torr
Vbmin=282
c2=2.718/pdmin
c1=Vbmin*c2/2.718
```

```
x=.0025:.0001:.008;
vb=(c1.*x)./(log(x)+log(c2));
figure(3)
subplot(2,2,1)
plot(x,vb,'r.-','linewidth',3)
hold on
d=.0366; %cm or 0.0144in
P=[53.4 83.8 101 152 205]; %% pressure in millitorr
P=P/1000;  %% pressute in torr
Vb=[338 314 304 282 324]; %% voltage in volts
pd=d*P;
plot(pd,Vb,'linewidth',3)
title('Paschen curve of thick wafer Baseline.')
xlabel('pd (torr-cm)')
ylabel('Vb')
legend('Expected','Data','Location','NorthEast')
grid on
hold on
scatter(pd,Vb)

%% 300um thick wafer
pdmin= 100*.0384  %millitorr
pdmin=pdmin/1000  %torr
Vbmin=234
c2=2.718/pdmin
c1=Vbmin*c2/2.718
x=.0016:.0001:.025;
vb=(c1.*x)./(log(x)+log(c2));
subplot(2,2,2)
plot(x,vb,'r.-','linewidth',3)
hold on
d=.0384; %cm or 0.0151in
P=[32.2 50.7 84.1 100 149 200 518]; %% pressure in millitorr
P=P/1000; %% pressute in torr
Vb=[382 320 284 234 262 276 348]; %% voltage in volts
pd=d*P;
plot(pd,Vb,'linewidth',3)
```

```
title('Paschen curve of thick wafer with 300um holes')
xlabel('pd (torr-cm)')
ylabel('Vb')
legend('Expected','Data','Location','SouthEast')
grid on
hold on
scatter(pd,Vb)

%% 400um thick wafer
pdmin= 102*.0285  %millitorr
pdmin=pdmin/1000  %torr
Vbmin=270
c2=2.718/pdmin
c1=Vbmin*c2/2.718
x=.0015:.0001:.016;
vb=(c1.*x)./(log(x)+log(c2));
subplot(2,2,3)
plot(x,vb,'r.-','linewidth',3)
hold on
d=.0285; %cm or 0.0112in
P=[30.3 51.3 83.7 102 150 203 498]; %% pressure in millitorr
P=P/1000; %% pressute in torr
Vb=[326 310 290 270 282 334 354]; %% voltage in volts
pd=d*P;
plot(pd,Vb,'linewidth',3)
title('Paschen curve of thick wafer with 400um holes')
xlabel('pd (torr-cm)')
ylabel('Vb')
legend('Expected','Data','Location','SouthEast')
grid on
hold on
scatter(pd,Vb)

%% 500um thick wafer
pdmin= 198*.0372  %millitorr
pdmin=pdmin/1000  %torr
Vbmin=282
```

```
c2=2.718/pdmin
c1=Vbmin*c2/2.718
x=.004:.0001:.02;
vb=(c1.*x)./(log(x)+log(c2));
subplot(2,2,4)
plot(x,vb,'r.-','linewidth',3)
hold on
d=.0372; %cm or 0.01465in
P=[30.7 50.6 83.1 98.2 149 198 498]; %% pressure in millitorr
P=P/1000; %% pressute in torr
Vb=[346 346 308 298 298 282 352]; %% voltage in volts
pd=d*P;
plot(pd,Vb,'linewidth',3)
title('Paschen curve of thick wafer with 500um holes')
xlabel('pd (torr-cm)')
ylabel('Vb')
legend('Expected','Data','Location','SouthEast')
grid on
hold on
scatter(pd,Vb)
```

B. MATLAB CODE USED TO GRAPH FIGURES 21-23 IN APPENDIX B

```
%% Thesis Data Comparison

clear all
close all
clc


%%%%Thinnest Wafers
%% Thinnest wafer Baseline
db=.0154; %cm or 0.00605in
Pb=[32.4 51.4 82.3 100 153 200 495]; %% pressure in millitorr
Pb=Pb/1000;  %% pressute in torr
Vbb=[366 310 286 280 282 320 346]; %% voltage in volts
pdb=db*Pb;
```

```
%% 300um thinnest wafer
d3=.0137; %cm or 0.00535in
P3=[35.2 51.3 82.2 103 151 202 509]; %% pressure in millitorr
P3=P3/1000; %% pressute in torr
Vb3=[326 292 262 244 252 260 302]; %% voltage in volts
pd3=d3*P3;
%% 400um thinnest wafer
d4=.0153; %cm or 0.00605in
P4=[32.1 52.9 82.9 98.3 154 204 517]; %% pressure in millitorr
P4=P4/1000; %% pressute in torr
Vb4=[364 310 276 264 254 276 348]; %% voltage in volts
pd4=d4*P4;
%% 500um thinnest wafer
d5=.0153; %cm or 0.00605in
P5=[35.1 50 83.8 102 148 199 500]; %% pressure in millitorr
P5=P5/1000; %% pressute in torr
Vb5=[316 284 266 256 264 326 364]; %% voltage in volts
pd5=d5*P5;
%% Comparison plot for thinnest wafers
figure(1)
plot(pdb,Vbb,'b.-','linewidth',3)
hold on
plot(pd3,Vb3,'go:','linewidth',2)
hold on
plot(pd4,Vb4,'rx-.','linewidth',2)
hold on
plot(pd5,Vb5,'k+--','linewidth',2)
hold on
grid on
title('Paschen curves of thinnest wafers.')
xlabel('pd (torr-cm)')
ylabel('Vb')
legend('Baseline','300um','400um','500um','Location','SouthEast')

%%%%Middle Wafers
%% Middle wafer Baseline
db=.0287; %cm or 0.0113in
```

```
Pb=[31.5 50.4 85.9 100 151 198 496]; %% pressure in millitorr
Pb=Pb/1000;  %% pressute in torr
Vbb=[386 374 340 328 312 312 386]; %% voltage in volts
pdb=db*Pb;
%% 300um Middle wafer
d3=.0303; %cm or 0.0119in
P3=[33.9 50.9 80.7 106 159 208 503]; %% pressure in millitorr
P3=P3/1000; %% pressute in torr
Vb3=[296 276 248 258 258 274 324]; %% voltage in volts
pd3=d3*P3;
%% 400um Middle wafer
d4=.0284; %cm or 0.01115in
P4=[31.8 48 84.3 107 152 200 500]; %% pressure in millitorr
P4=P4/1000; %% pressute in torr
Vb4=[332 318 284 280 284 298 360]; %% voltage in volts
pd4=d4*P4;
%% 500um Middle wafer
d5=.026; %cm or 0.01025in
P5=[31.7 56.6 81.4 101 150 200 499 800]; %% pressure in millitorr
P5=P5/1000; %% pressute in torr
Vb5=[322 290 260 250 272 318 300 340]; %% voltage in volts
pd5=d5*P5;
%% Comparison plot for Middle wafers
figure(2)
plot(pdb,Vbb,'b.-','linewidth',3)
hold on
plot(pd3,Vb3,'go:','linewidth',2)
hold on
plot(pd4,Vb4,'rx-.','linewidth',2)
hold on
plot(pd5,Vb5,'k+--','linewidth',2)
hold on
grid on
title('Paschen curves of middle wafers.')
xlabel('pd (torr-cm)')
ylabel('Vb')
legend('Baseline','300um','400um','500um','Location','SouthEast')
```

```
%%%%Thick Wafers
%% Thick wafer Baseline
db=.0366; %cm or 0.0144in
Pb=[53.4 83.8 101 152 205]; %% pressure in millitorr
Pb=Pb/1000;  %% pressute in torr
Vbb=[338 314 304 282 324]; %% voltage in volts
pdb=db*Pb;
%% 300um Thick wafer
d3=.0384; %cm or 0.0151in
P3=[32.2 50.7 84.1 100 149 200 518]; %% pressure in millitorr
P3=P3/1000; %% pressute in torr
Vb3=[382 320 284 234 262 276 348]; %% voltage in volts
pd3=d3*P3;
%% 400um Thick wafer
d4=.0285; %cm or 0.0112in
P4=[30.3 51.3 83.7 102 150 203 498]; %% pressure in millitorr
P4=P4/1000; %% pressute in torr
Vb4=[326 310 290 270 282 334 354]; %% voltage in volts
pd4=d4*P4;
%% 500um Thick wafer
d5=.0372; %cm or 0.01465in
P5=[30.7 50.6 83.1 98.2 149 198 498]; %% pressure in millitorr
P5=P5/1000; %% pressute in torr
Vb5=[346 346 308 298 298 282 352]; %% voltage in volts
pd5=d5*P5;
%% Comparison plot for Thick wafers
figure(3)
plot(pdb,Vbb,'b.-','linewidth',3)
hold on
plot(pd3,Vb3,'go:','linewidth',2)
hold on
plot(pd4,Vb4,'rx-.','linewidth',2)
hold on
plot(pd5,Vb5,'k+--','linewidth',2)
hold on
grid on
title('Paschen curves of thick wafers.')
```

```
xlabel('pd (torr-cm)')
ylabel('Vb')
legend('Baseline','300um','400um','500um','Location','SouthEast')
```

THIS PAGE INTENTIONALLY LEFT BLANK

LIST OF REFERENCES

1. Nasser, Essam, *Fundamentals of Gaseous Ionization and Plasma Electronics,* John Wiley & Sons, Inc., 1971.

2. Biblarz, Oscar and Bell, W. J., “Thermionic Arc Breakdown in Small Discharge Gaps: Model and Application," IEEE Transactions on Industry Applications, Vol 34, No 2, March/April 1998, pp 325-331.

3. Sinibaldi, Jose and Biblarz, Oscar, "Thermionic Ion Propulsion (TIP) Concept," Proposal sumitted to DARPA, 2003.

4. Biblarz, Oscar and Sinibaldi, Jose, "Study of DC Ion Thrusters with Argon Propellants," Abstract submitted to the AIAA-JPC, Sacramento, CA, 2006.

5. Sutton, G. P. and Biblarz, Oscar, *Rocket Propulsion Elements,* VIIth Edition, Wiley, NY, 2001.

6. Penache, Maria C., "Study of High Pressure Glow Discharges Generated by Micro-Structured Electrode (MSE) Arrays," PhD Dissertation, Frankfurt am Main University, Germany, 2002.

7. Perry, Frank H. Jr., "Apparatus for Study of Ion Thruster Propellant Ionization," Master’s Thesis, Naval Postgraduate School, Monterey, California, December, 2006.
8. Wright, Mike, “ION PROPULSION: Over 50 Years in the Making.” [http://science.nasa.gov/newhome/headlines/prop06apr99_2.htm]. Nov 06.

9. Wikipedia, “Ion Thruster.” [http://en.wikipedia.org/wiki/Ion_thruster]. Nov 06.

THIS PAGE INTENTIONALLY LEFT BLANK

INITIAL DISTRIBUTION LIST

1. Defense Technical Information Center
   Ft. Belvoir, Virginia

2. Dudley Knox Library
   Naval Postgraduate School
   Monterey, California

3. Head, Information Operations and Space Integration Branch, PLI/PP&O/HQMC,
   Washington, DC

4. Professor Oscar Biblarz
   Department of Mechanical and Astronautical Engineering
   Naval Postgraduate School
   Monterey, California

5. Professor Jose O. Sinibaldi
   Department of Mechanical and Astronautical Engineering
   Naval Postgraduate School
   Monterey, California

6. Provost, Dr, Leonard Ferrari
   Naval Postgraduate School
   Monterey, California

7. Dean of Research
   Research Office
   Naval Postgraduate School
   Monterey, California